Chapter 2

LONG-TERM CHANGES

M. Van Roozendael and G. Vaughan

Contributing Authors
A. Engel, S. Godin, H. Jäger, E. Kyrö, B. Naujokat, C. Schiller, A. Weiss and R. Zander

HIGHLIGHTS

This section summarises the main scientific highlights arising from recent research activities in Europe on the issue of the long-term variability and change of stratospheric composition and meteorology. The bullet list below is meant to provide an overview of the European contribution to the subject. More complete and detailed scientific highlights including results from non-European researchers can be found in the recent WMO Scientific Assessment of Ozone Depletion: 1998, and SPARC Ozone and Water Vapour Assessments [Harris et al., 1998; Kley et al., 2000].

Ozone

- High quality long-term Dobson records in Europe show that total ozone declined after 1980 during all seasons, but especially in the January-April period. Recent measurements show that northern hemisphere total ozone has increased slightly in the last few years, although values are still below pre-1975 levels. The ozone hole in Antarctica continues unabated.

- The determination of ozone trends on the global scale relies on satellite measurements validated by ground-based observations. A European contribution to ozone monitoring from space became available in July 1995 with the Global Ozone Monitoring Experiment (GOME) onboard the ERS-2 platform, partly filling the gap from late 1994 to 1996 in the TOMS data record. The combined TOMS (N7, M3 and EP) and GOME satellite data set allows the latitudinal distribution of the O_3 trends over the period 1979-2000 to be documented. These are largest for high latitudes in winter and overall statistically insignificant in the tropics. Current differences of the order of 5-15 DU between GOME, TOMS and ground-based total ozone measurements still need to be resolved to allow reliable assessment of changes in trend after 1995 in comparison to the pre-Pinatubo trend.

- Altitude resolved O_3 trend analysis based on satellite and ozone sondes observations show the largest downward trend (approximately –7% per decade) arising in the upper stratosphere around 40 km altitude and in the lowermost stratosphere around 16 km. Recent re-evaluation of ground-based Umkehr observations available since the beginning of the sixties confirm the trend reported for the upper stratosphere. In the lowermost stratosphere, the derived trends are sensitive to the period chosen for analysis, and decrease substantially when the most recent years are included.

Stratospheric composition

- The total amount of organic chlorine (CCl_y) contained in long- and shorter-lived chlorocarbons reached maximum values of 3.6±0.1 ppbv between 1993 and 1994 and is beginning to decrease slowly in the troposphere mainly due to reduced emissions of methyl chloroform (CH_3CCl_3).

- The loading of inorganic chlorine in the stratosphere, monitored since 1977 at the Jungfraujoch (Switzerland), reached a maximum around 1997, consistent with the reduction in emissions of important organic chlorine species achieved by international regulations (Montreal Protocol and its Amendments and Adjustments).

- Evaluations of the bromine budget in the stratosphere by two different methods provide evidence that stratospheric inorganic bromine has increased by about 25% during the decade 1987-1996. This increase consistently follows the measured trend in tropospheric source gases, which is primarily due to the increase in atmospheric halons H-1211, H-1301, H-2402 and H-1201. Continued increase of halons over the next few years could cause the abundance of equivalent chlorine to decline more slowly than predicted.

- A significant increase in the stratospheric water vapour concentration has been identified over recent decades. The European measurement record of H_2O, available since the 1990s, and that of other hydrogen species will become sufficiently large within the next few years to follow the current changes.

- The column abundance of CH_4, monitored at the Jungfraujoch since 1950, has increased by 35% over the last fifty years but with a declining rate of growth during the last few years, in line with findings from *in situ* surface measurements of CH_4.

- An upward trend in NO_2 column of about 5% per decade has been identified at the Jungfraujoch (Switzerland) during the last two decades. This increase, which is similar to the trend recently reported at Lauder (New Zealand), is about twice the trend in tropospheric N_2O, the principal source of stratospheric NO_2. Recent 2-D model calculations indicate that the difference could be explained by a long-term change in the NO_x/NO_y partitioning due to an overall effective decrease of about 20% of the stratospheric aerosol loading between 1980 and 1998 related to the El Chichon and Mt Pinatubo volcanic eruptions.

- The two most recent major volcanic eruptions, El Chichon (1982) and Mt Pinatubo (1991) temporarily increased sulphate aerosol abundances by more than an order of magnitude. On the other hand, backscatter lidar observations of stratospheric sulphate aerosol at Garmisch-Partenkirchen (Germany) show no clear trend from 1976-2000, indicating that any anthropogenic contribution must be smaller than thought in the previous EC report.

Temperature and dynamics

- Trends in stratospheric temperatures between 100 and 30 mb, derived from northern hemisphere radio sonde analyses available since 1965, are negative at all latitudes being greatest in the subtropics and polar regions around 50 mb, where they exceed –0.7 K per decade. Calculated temperature trends strongly depend on the beginning and end dates considered for the analysis, especially in the highly variable winter stratosphere. For the

North Pole, Freie Universität Berlin (FUB) analyses at 30 mb from 1955-2000 show no significant trend for the whole period in March, but a strong cooling (–6 K per decade) since 1979. The same data set for July (when the inter-annual variability is much less) exhibit a significant overall cooling of 0.6 K per decade from 1955-2000 and 1.3 K per decade since 1979.

- Processes driving the natural variability of the northern hemisphere stratosphere are now better understood. In particular, the role of the Quasi-Biennial Oscillation (QBO) in stabilising the polar vortex during its westerly phases and in disturbing it during its easterly phases has been elucidated. Moreover the role played by the solar cycle in modulating this connection has been further established. It has also been shown that warm events of the El Niño/Southern Oscillation (ENSO) often result in major mid-winter warmings, while strong volcanic eruptions like Mt Pinatubo (1991) result in a warming of the tropical stratosphere.

- New evidence has been found that the frequency of events mixing subtropical ozone-poor air into the mid-latitude stratosphere may have increased over the past twenty years, possibly explaining some of the observed ozone changes in northern mid-latitude regions.

- Significant progress has been achieved in characterising the polar vortex climatology, again based on ECMWF meteorological analyses covering the period 1979-2000. Results indicate that the polar vortices of the 1990s have been stronger and of longer duration than those in the 1980s, in accordance with the reported long-term cooling of the polar stratosphere.

- The North Atlantic Oscillation (NAO) and Arctic Oscillation (AO) are important components of long-period variability in the atmosphere, with the AO in particular being closely linked to the strength of the polar vortex. Recent GCM model experiments emphasise that a correct representation of the AO/NAO mode of variability is important to correctly represent the atmospheric response to stratospheric aerosol, stratospheric ozone loss, changes in solar activity, and increased greenhouse gas forcing.

2.1 INTRODUCTION

This chapter is concerned with two issues: changes in the abundance of trace species and aerosols, and long-term changes in meteorological conditions in the stratosphere. Both these factors impact on ozone, since its distribution results from a balance between chemistry and transport. In the extra-tropical lower stratosphere in particular, where there appear to be significant ozone trends [Harris et al., 1998], the ozone concentration is very sensitive to changes in circulation – both in the wave driven meridional circulation of the main stratosphere (the Brewer-Dobson circulation) and the isentropic mixing across the tropopause driven by synoptic scale dynamics in the troposphere. A thorough understanding of such changes is needed if the anthropogenic component of observed ozone changes is to be identified. In this chapter we present an update on the changes observed in stratospheric composition, temperature and circulation since the 1950s together with new work made possible by the ECMWF ERA-15 re-analyses. Together, they provide the backdrop against which changes in ozone must be interpreted. They also allow the dynamical changes themselves to be examined for trends (possibly linked to anthropogenically-forced climate change) and low-frequency oscillations in the atmosphere and oceans, for example the solar cycle, QBO and AO.

During recent decades, concern about the erosion of the ozone layer has led to reductions in the anthropogenic emissions of several halogen bearing source gases with large Ozone Depletion Potentials (ODPs), as identified in the Montreal Protocol (1987) and its subsequent Amendments and Adjustments. This has had a notable influence on the chlorine loading of the stratosphere, which has been the primary cause of ozone layer depletion at the spring poles. European contributions to long-term change investigations in the stratosphere have resulted mainly from involvements in the Network for the Detection of Stratospheric Change (NDSC) and from the investigation of individual data sets gathered during stratospheric balloon flights. This chapter summarises the salient results of these investigations.

Since the last EC assessment in 1996, the stratosphere has experienced a period of very low aerosol abundance; the perturbation due to Mt Pinatubo has decayed away and aerosol loadings are now at their lowest level recorded since the late 1970s. In addition, the period has been one of very marked inter-annual variability at high latitudes, with two very warm winters (1997/98 and 1998/99) followed by one of the coldest on record (1999/2000). Such inter-annual variability means that very long records (or very large changes) are needed before statistically significant trends in temperature, circulation and chemical composition can be discerned from noise; the same is necessarily true for ozone.

2.2 CHANGES IN OZONE

This section considers only the observational evidence for ozone changes. Interpretation and trend analysis are presented in Chapter 4. For a fuller description of the methods used to measure ozone and of the observed trends, see Staehlin et al. [2001].

2.2.1 Ground-based measurements of total ozone

The first observational evidence of long-term changes to the ozone layer came from the Dobson spectrophotometer measurements at Halley Bay, Antarctica (76°S). The drastic reduction in total ozone during spring [Farman et al., 1985] alerted the scientific community and the general public to the existence of the ozone hole and set in train an extensive research and monitoring effort to understand the changes. The monthly mean total ozone at Halley Bay for each October from 1955-2000 is shown in Figure 2.1, clearly demonstrating the development of the ozone hole after 1975 with a levelling off of the October mean values in recent years. Ozone sonde measurements from Antarctica in the 1990s [Hofmann et al., 1997] show almost complete destruction of the ozone layer between 14 and 18 km by mid-October, with significant depletion between 12 and 22 km.

Away from Antarctica the changes in total ozone are smaller, and are marked by considerable natural variability. The longest total ozone record in existence is that for Arosa, Switzerland [Staehelin et al., 1998]. This is shown in Figure 2.2 for three separate four-month periods. In each case no systematic change in ozone can be discerned from the noise before about 1980. Since then, total ozone has declined at all times of the year, with the greatest decrease (~30 DU) in the January-April period. In the last few years, total ozone has increased a little, although values remain below the pre-1975 mean.

Confirmation that the decline in total ozone in northern mid-latitudes occurred at all longitudes, and was not peculiar to the European sector, is provided by Figure 2.3. This shows the deviation of total ozone in winter from the long-term pre-1976 average for three longitude

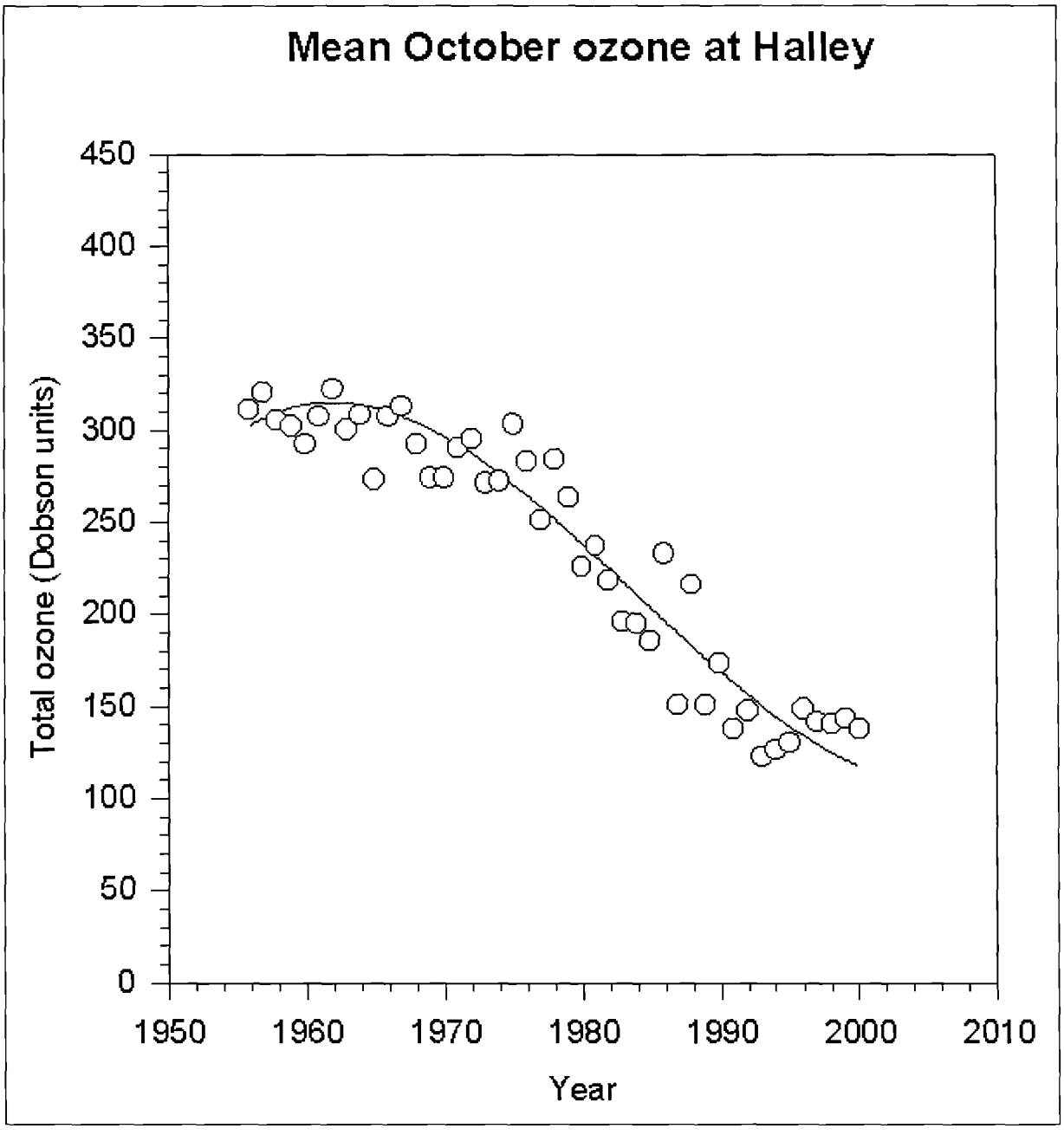

Figure 2.1 *October mean total ozone measured by Dobson spectrophotometer at Halley Bay (76°S) from 1955 to 2000. [Updated from Farman et al., 1985 and Jones and Shanklin, 1995].*

sectors; it is based on a composite of quality controlled ground-based observations and TOMS satellite measurements [Bojkov et al., 1998, 2000]. A similar picture to Figure 2.2 is found at all longitudes: a decline of ~8% in the 1980s to a minimum in 1992, followed by a slight increase in the 1990s.

Investigation of trends in total ozone and future identification of the recovery of the ozone layer require high quality and consistent long-term total ozone data from ground-based networks. For the Dobson part of the total ozone monitoring network in Europe, a Regional Dobson Calibration Center (RDCC) has been established and started to function in 1999. The RDCC is a joint operation by the Meteorological Observatory at Hohenpeissenberg (Germany)

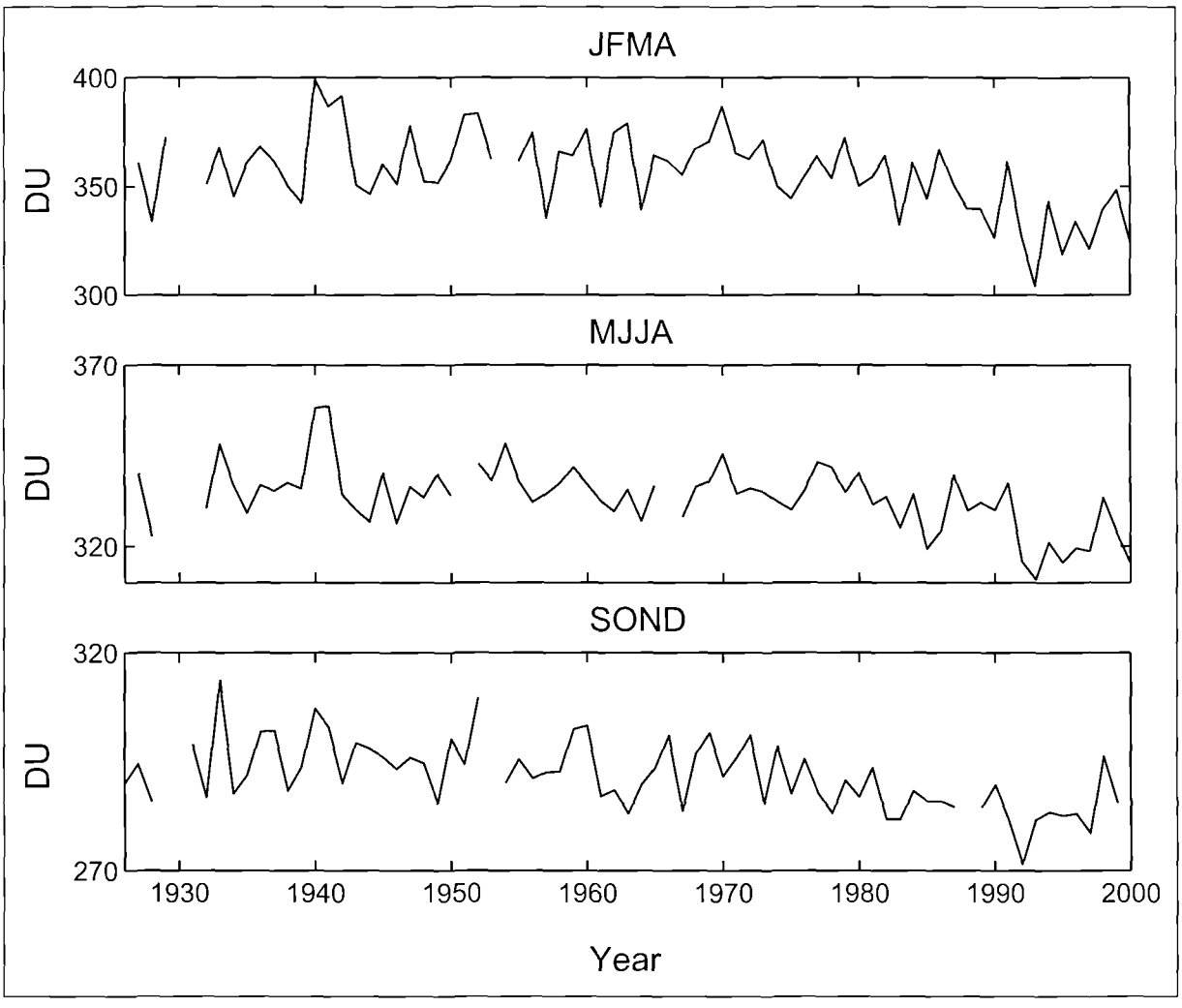

Figure 2.2 *Total ozone measured by Dobson spectrophotometer at Arosa, Switzerland, from 1926 to the present [updated from Staehlin et al., 1998]. Data have been averaged over four-monthly intervals for each year.*

and the Solar and Ozone Observatory at Hradec Kralove (Czech Republic). Its activities are linked with the GAW program of WMO and with the World Dobson Calibration Center, at NOAA-CMDL, Boulder, Colorado.

2.2.2 Satellite measurements of total ozone

Ground-based measurements of total ozone are relatively scarce outside northern mid-latitudes, and to extend Figure 2.3 to other latitude zones we must rely on satellite measurements. Regular total ozone measurements from satellites began in October 1978 with the Nimbus 7 TOMS (N7), which operated until 1993 [Heath et al., 1975; McPeters et al., 1996]. The TOMS series has been continued by instruments on the satellites METEOR-3 (M3, 1991-4), ADEOS (1996/97) and Earth Probe (EP, 1996 to the present). This frequent change of instrument in the 1990s (together with a data gap between November 1994 and June 1996) introduces some uncertainty into long-term changes derived from TOMS. A European contribution to ozone monitoring has become available in recent years from the GOME on ERS-2 [Burrows et al., 1999]. This has operated since July 1995, partly filling the gap in the TOMS data record.

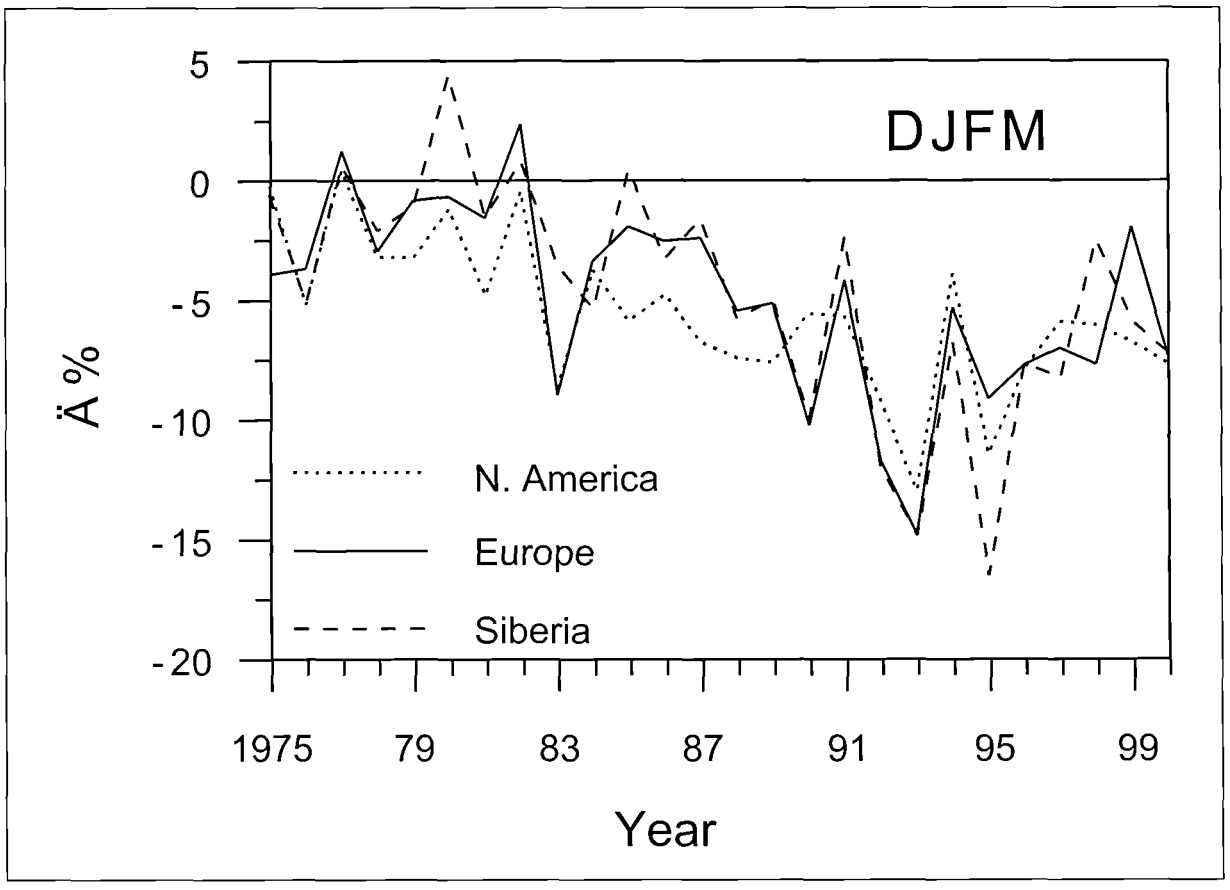

Figure 2.3 *Area-averaged (45-65°N) total ozone departures (in %) from the long-term pre-1976 averages for December-March 1979-2000. The 2σ error for each point is less than 6%. [Bojkov et al., 1998, 2000].*

The satellite measurements are summarised in Figure 2.4. This shows the average total ozone over 30° latitude bands in winter and summer for the period 1979-2000 derived from the N7, M3 and EP TOMS instruments; also shown are corresponding GOME measurements beginning in 1995. None of the satellites can measure in the dark, so the values shown for high latitudes in winter are not as reliable as for the other panels. The TOMS data show an overall decline in ozone at all latitudes in both seasons. In the tropics the overall trend is small (<0.2 DU yr^{-1}) and statistically insignificant since there is considerable decadal scale variability. Little overall trend is evident in the northern hemisphere summer, but in the winter months a steady decline is clear in mid-latitudes (about 2 DU yr^{-1}) and a very obvious change is seen at high latitudes around the time of the Mt Pinatubo eruption in 1991, with recovery to the long-term trend in 1998 and 1999. In southern mid-latitudes the decline is marked in both seasons (at 1.0-1.5 DU yr^{-1}) and not surprisingly very obvious at high latitudes in JAS. Minimum total ozone values below 100 DU have been measured in the ozone hole in the 1990s, while its maximum area (defined as that within the 220 DU contour) continues to increase [WMO, 1999].

The data gap in the TOMS data record between 1994 and 1996 has led to some difficulties in assessing the continuation of the observed long-term trend after 1994. According to the most recent WMO assessment [WMO, 1999 Figure 4.12], the average total ozone between 60°N and 60°S from N7 and EP TOMS (after removing variability due to season, solar cycle, and QBO) show an increase from 1994 to 1998, while Dobson measurements similarly filtered showed no

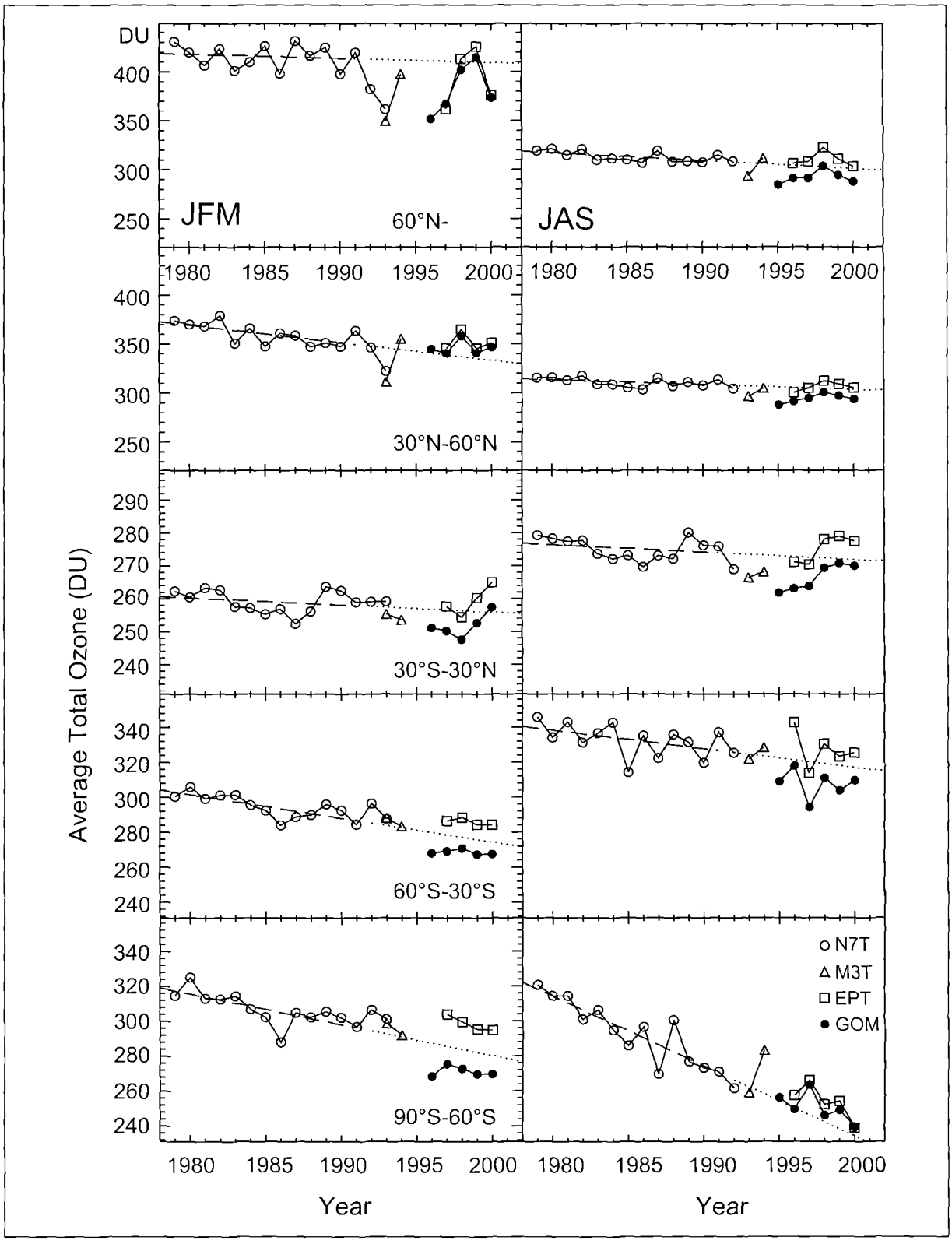

Figure 2.4 *Average total ozone for three-month periods (left column: January, February, March; right column: July, August, September) for each year between 1978 and 2000. The data are divided into 30° latitude bands, with the tropics taken as one. Different symbols denote measurements from Nimbus-7 TOMS (open circles), Meteor-3 TOMS (open triangles), Earth Probe TOMS (open squares) and GOME (filled circles). Note that the satellites cannot sample uniformly at high latitudes in winter as they rely on backscattered sunlight for their measurements. The regression lines represent the linear fit to the pre-Pinatubo data. Extrapolation of this linear regression to the period after 1991 is indicated by the dotted line for reference purpose. [Updated from Burrows et al., 2000].*

change. Nevertheless, both data sets indicate that the downward trend prior to Pinatubo has not continued. In order to determine whether such changes are real, the issue of data quality has to be addressed.

From Figure 2.4 it is apparent that systematic deviations between the GOME V2.7 and TOMS V7 data exist. Comparison of GOME data with 76 NH Dobson stations showed that deviations are dependent on season. During spring a positive bias of GOME of about 1-2% is observed, which changes to about –3% in autumn [update from Burrows et al., 2000]; however, the average difference over four years is less than 0.5%. A similar seasonal pattern (shifted by half a year) is observed in the southern hemisphere [Bodeker et al., 2001]. EP TOMS total ozone data has a positive bias of about 1.5% in the northern hemisphere in all seasons [Burrows et al., 2000]. There is an apparent north-south asymmetry in the differences between EP TOMS and Dobson data [Lambert et al., 1999]. At 50°N the bias is about 6 DU on average, while at 50°S this bias increases to about 12 DU [Bodeker et al., 2001]. By using Dobson data as a transfer standard, it was estimated that EP TOMS measures between 2 and 6 DU more than Nimbus 7 TOMS, depending on the latitude [Bodeker et al., 2001].

At least another decade of global satellite measurements is needed to confirm any changes in the long-term ozone trend, taking into account instrumental issues and other uncertainties as discussed in more detail in Chapter 4.

2.2.3 Changes in the ozone vertical profile

A detailed assessment of changes in ozone vertical profiles has been published by SPARC [Harris et al., 1998]. This assessment concluded that only four measurement techniques have produced records long enough to assess long-term changes: the satellite instruments SAGE (1 and 2) and SBUV, balloon-borne ozone sondes and the ground-based Umkehr method (which uses zenith-sky observations from the Dobson spectrophotometer at twilight). Below 20 km, ozone sondes alone were considered sufficiently accurate to derive changes, whereas from 20-50 km Umkehr and satellite data could also be used. Harris et al. [1998] concluded that, between 1980 and 1996, ozone losses were statistically significant at all altitudes between 12 and 50 km, and that there were two regions of maximum decrease: the upper stratosphere around 40 km and the lowermost stratosphere around 16 km. In both these regions a change of approximately –7% per decade in ozone concentration has been observed, separated by a layer in the mid-stratosphere (~25-35km) where the decrease was less than 3% per decade.

A recent European project called REVUE (Reconstruction of Vertical ozone distribution from Umkehr Estimates) has re-evaluated the long-term global Umkehr record, which goes back to the beginning of the sixties for some stations [Godin et al., 2000]. Using an improved Umkehr algorithm and a global aerosol climatology, a homogeneous data set of ozone vertical profiles was derived for 14 Umkehr stations. This data set showed improved agreement with satellite and ozone sonde data, especially in the lower stratosphere. Results are shown for European mid-latitude stations (Belsk, Observatoire de Haute Provence and Arosa) in Figure 2.5, as linear trends over two periods: 1978-1997 and 1978-1999. Also shown on this diagram are the corresponding trends derived from Payerne ozone sondes. The Umkehr inversion algorithm reports ozone values in Umkehr layers. These layers are approximately 5 km thick and are centered at the layer number times 5 km in height. Also shown on this diagram are the corresponding trends derived from ozone sondes. The Umkehr shows a consistent trend of –5% per decade in the upper stratosphere (layers 7-8) but a much smaller negative trend than

the sondes in the lower stratosphere. Note in particular the sensitivity of the derived trend to the period chosen for analysis, with the inclusion of 1998 and 1999 resulting in much smaller trends near the tropopause, particularly in the ozone sonde data. This point is further discussed in Chapter 4.

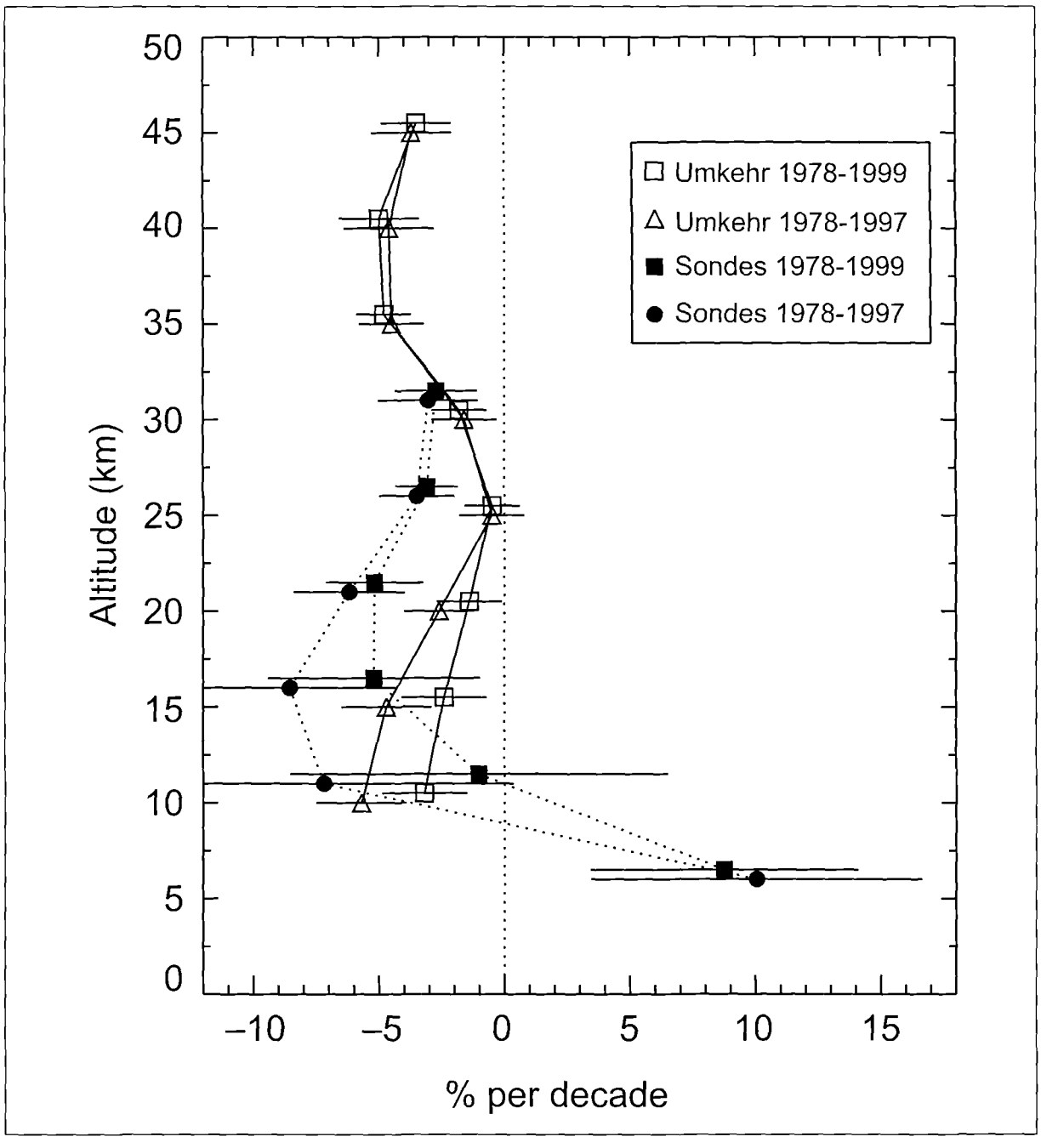

Figure 2.5 *Average trends in ozone vertical profiles between 1978 and the present, for European stations: Belsk, OHP and Arosa in the case of Umkehr, Payerne for the ozone sondes. [Godin et al., 2000].*

2.3 LONG-TERM CHANGES IN HALOGEN SPECIES

2.3.1 Chlorine species

As noted in Section 2.1, the emissions into the atmosphere of chlorine-containing chemicals with large ODPs (primarily all CFCs) have been reduced substantially in recent years. Chlorine source gases and resulting reactive chlorine species have been measured regularly both from the ground and from balloons by remote sensing and *in situ* techniques. However, only a few of these data sets have sufficient temporal coverage to allow a determination of long-term changes.

Surface measurements of the long- and shorter-lived halogenated sources gases contributing to the total organic chlorine loading of the atmosphere (CCl_y) have been provided since the late 1970s by two major global ground-based *in situ* networks: the ALE/GAGE/AGAGE network [Prinn et al., 1998] and the NOAA/CMDL network [Elkins et al., 2000]. The total CCl_y is defined as the sum of the chlorine atoms bound in all organic chlorine-bearing gases released to the atmosphere. As none of the monitoring networks measures all species making up CCl_y, it is in practice evaluated from available measurements of the dominant Cl-bearing organic species. For example, the ALE/GAGE/AGAGE network has estimated the fraction CCl_y* of total CCl_y which can be inferred from the principal chlorocarbons CFC-11, -12, and -113, methyl chloroform (CH_3CCl_3) and carbon tetrachloride (CCl_4). Figure 2.6 shows a recent update of the time series of measurements collected for these species since 1986 at the Mace Head station in Ireland [Derwent et al., 2001]. When augmenting these data with contributions from the constant natural source of methyl chloride (CH_3Cl) and other minor species, it can be estimated that the global peak of CCl_y occurred between 1993 and 1994 at a level equal to 3.6±0.1 ppbv [Montzka et al., 1996, Cunnold et al., 1997]. As can be seen in Figure 2.6, the subsequent CCl_y decline was primarily due to the decrease in CH_3CCl_3 [see also Montzka et al., 1996; Prinn et al., 1995]. Similar results have been obtained from both AGAGE and NOAA/CMDL networks. Further analysis actually shows that the international implementation of the Montreal Protocol on Substances that Deplete the Ozone Layer and its Amendments has resulted in bringing the amounts of most CFCs and chlorocarbons in the atmosphere down to amounts that are consistent with the Protocol's provisions regarding production and emission [WMO, 1999].

Complementary to ground-based *in situ* measurements, an approach actively pursued in Europe since 1978 to derive the temporal trend of CCl_2F_2 (CFC-12) in the lower stratosphere is the use of *in situ* observations of trace gases in the stratosphere by balloon-borne whole air samplers [Engel et al., 1998]. These are shown in Figure 2.7, where nitrous oxide (N_2O) is used as a vertical coordinate in order to remove the effect of dynamical processes in the individual profiles. The calculated trend of CFC-12 in the lowermost stratosphere follows the observed tropospheric increase very closely. However, the observed mixing ratios in the lowermost stratosphere appear to lag the global mean tropospheric trend by about one year. The most recent observations indicate that the slowing of the tropospheric increase has propagated into the lowermost stratosphere. While CFC-12 increased in the lowermost stratosphere at an average rate of 18.5±1.8 pptv per year between 1978 and 1990, the growth rate decreased to 8.9±3.8 pptv per year between 1990 and 2000 [updated from Engel et al., 1998]. From 1997 to present, the observed rate further decreased to 3±1.1 pptv per year. At higher altitudes the decrease in growth rates is less pronounced due to the time delay associated with the transport of tropospheric air to these altitudes. The increase observed at the 250 ppbv N_2O level (about 19 km at mid-latitudes) dropped from 12.9±1.5 pptv per year for the period 1978-1990 to 9.3±2.6 pptv per year for the period 1990-2000. The increase observed at this altitude after 1997 was only 5.6±3.5 pptv per year.

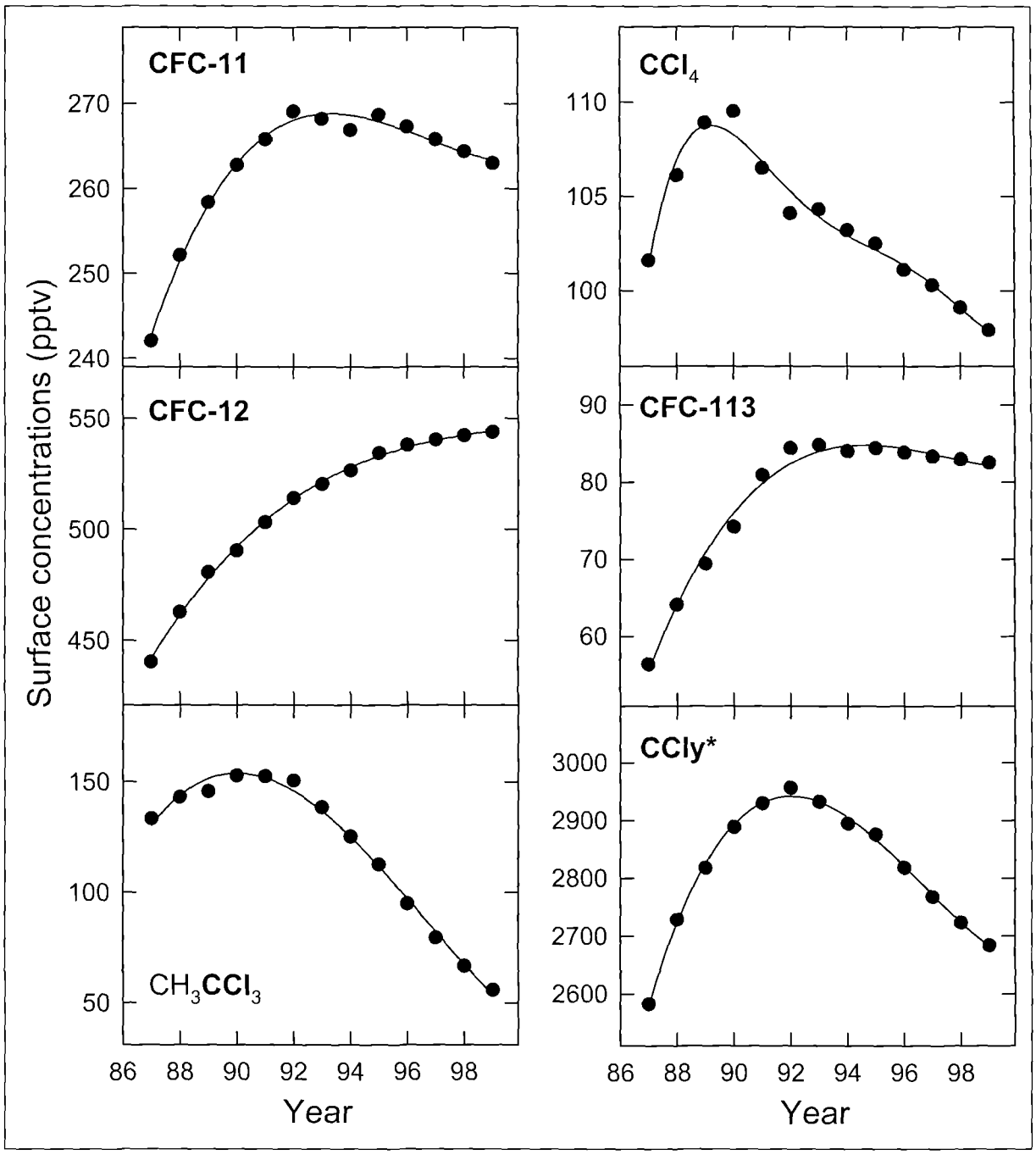

Figure 2.6 *Yearly averaged measurements of the surface concentrations of the principal chlorocarbons CFC-11, -12, and -113, CH_3CCl_3 and CCl_4 at the Mace Head station (Ireland) since 1986 [Derwent et al., 2001]. Also shown, the corresponding estimate of the tropospheric CCl_y* (see text). For total CCl_y, add about 650 pptv for the unmeasured species CH_3Cl and other minor contributors. Curves through data points are high-order polynomial regression lines.*

A method to evaluate the time lag due to transport of air between the troposphere and the stratosphere is to calculate the age of the stratospheric air. This can been derived from observations of the stable long-lived species SF_6 [Strunk et al., 2000], thus enabling the propagation of tropospheric trends into the stratosphere to be calculated [Engel et al., 2001]. Using a parameterisation for the width of the age spectrum these calculations show that at mid-latitudes the maximum chlorine loading at 13 km altitude was reached in 1995 with about

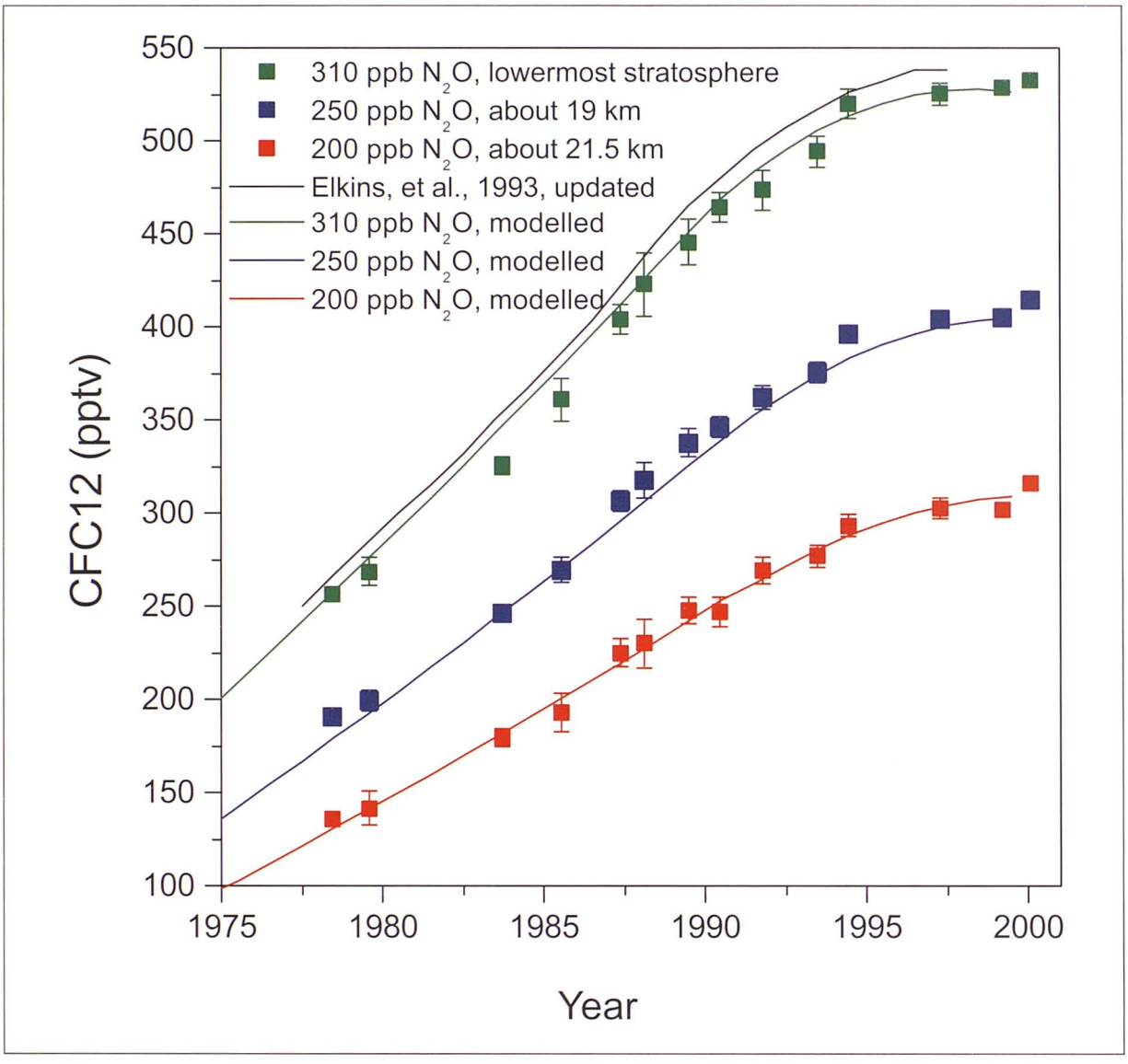

Figure 2.7 *Trends of CFC-12 for various altitudes in the stratosphere, updated from Engel et al. [1998]. The trends have been calculated relative to N_2O in order to eliminate short-term dynamical variability.*

3.6 ppbv of chlorine, while at 27 km altitude this is expected to happen about five years later with the maximum being at about 3.5 ppbv, as shown in Figure 2.8. As the mean time needed to transport air from the troposphere to a given location in the stratosphere increases with altitude (as can be seen from observation of the age of air), a time delay of about 3-4 years between the column maximum of Cl_y and the tropospheric maximum of CCl_y is expected. However, this contradicts the Cl_y-related observations in the upper stratosphere (where the time delay should be larger) by the UARS-HALOE experiment [Anderson et al., 2000] which show the maximum concentration of HCl at 55 km altitude to have occurred at about the same time (early 1997) as the maximum of the Cl_y column. The reason for the observation of a very early and very sharp maximum in HALOE HCl at 55 km is currently not understood [see also Waugh et al., 2001].

Both short-term, seasonal and secular characteristics observed by FTIR spectrometry in the vertical column abundances of HCl and HF above the northern mid-latitude NDSC station of the Jungfraujoch (46.5°N, 8.0°E, 3580 m asl) have been reported for the period 1977-1995 in the previous EC Report [1997, Figure 4.1, pp. 109] and in Zander et al. [1996]. In addition,

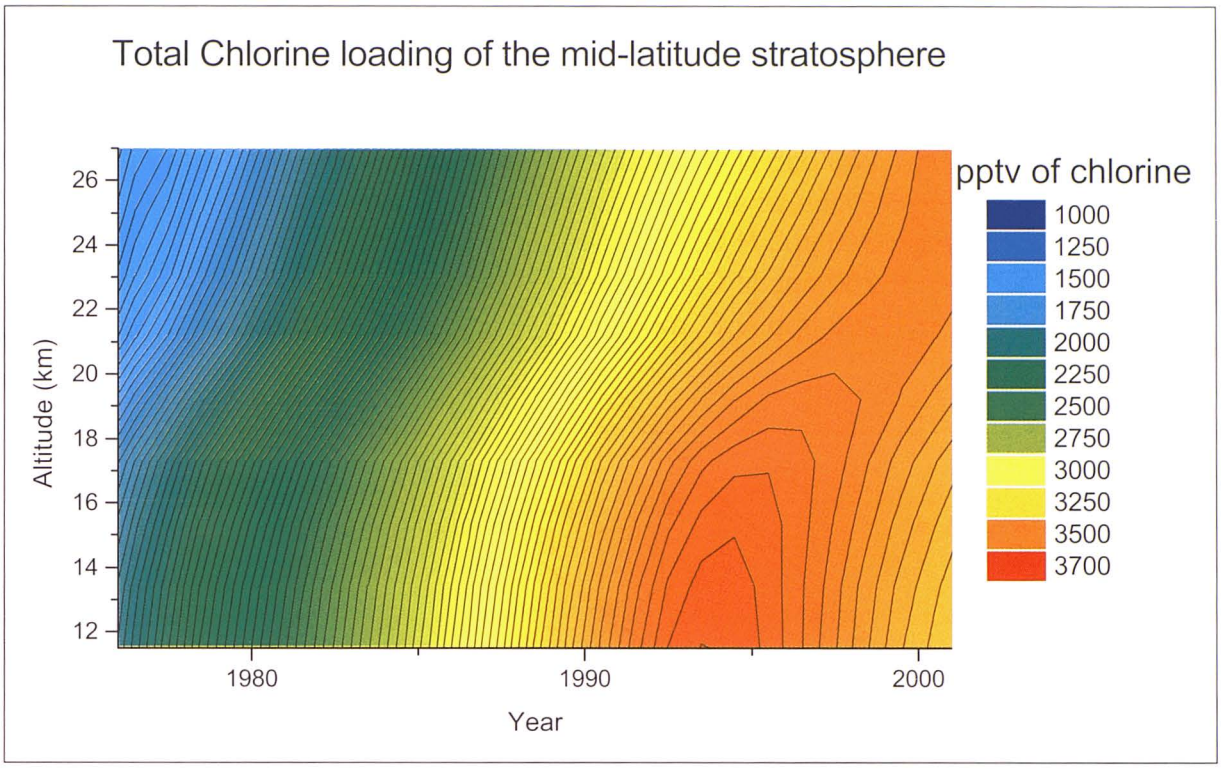

Figure 2.8 *Calculated evolution of the total chlorine loading of the stratosphere, based on tropospheric trends of CFCs-11, -12, -113, HCFC-22, CCl_4, and CH_3CCl_3 measured by NOAA-CMDL [updated from Elkins et al. 1993; Montzka et al., 1996] and SF_6-derived age of stratospheric air [Strunk et al., 2000]. CH_3Cl is included at a constant mixing ratio of 600 pptv.*

$ClONO_2$, NO, NO_2, HNO_3, HF, COF_2, O_3 and a series of source gases, such as N_2O, CH_4, CCl_2F_2 and $CHClF_2$, are monitored routinely as part of the University of Liège (ULg) contribution to NDSC. They include the most important constituents contributing to the budgets of inorganic chlorine (Cl_y = HCl + $ClONO_2$ + ClO + Cl_2O_2 + HOCl + OClO + 2x[Cl_2O_2] + COClF + BrCl +...) and fluorine (F_y = HF + 2x[COF_2] + COClF), the nitrogen family (NO_y = NO + NO_2 + N_2O_5 + HNO_3 + $ClONO_2$ + HNO_4 + NO_3...) as well as tracers of atmospheric transport/dynamics. Figure 2.9 reproduces the 1990-2000 daily mean vertical column abundances for eight of these. Since the mid-1990s, special attention was devoted to the secular evolution of the inorganic Cl_y budget, based on column measurements of HCl and $ClONO_2$ whose sum represents more than 92% of Cl_y at northern mid-latitudes [Mahieu et al., 2000]. As shown in Figure 2.10, the resulting Cl_y column abundance above the Jungfraujoch has stabilised around 1996-1997, and started to decrease thereafter. The peak Cl_y occurrence around 1996/97 is consistent with the maximum concentration of organic chlorine in the troposphere that was observed between 1993/94 [Montzka et al., 1996, Cunnold et al., 1997] also see Figure 2.6. It contradicts the Cl_y-related observations in the upper stratosphere by the UARS-HALOE experiment [Anderson et al., 2000] which show the maximum concentration of HCl at 55 km altitude to have occurred at about the same time (early 1997), although one would expect it to be delayed at upper altitudes by the mean age of air.

It must be stressed finally that the most important inorganic chlorine compounds (HCl and $ClONO_2$) show strong variability, as well as pronounced seasonal cycles. This is especially true at high latitudes during winter. Figure 2.11 displays the seasonal modulation of the HCl vertical column abundance observed by FTIR absorption spectrometry at the primary NDSC station of

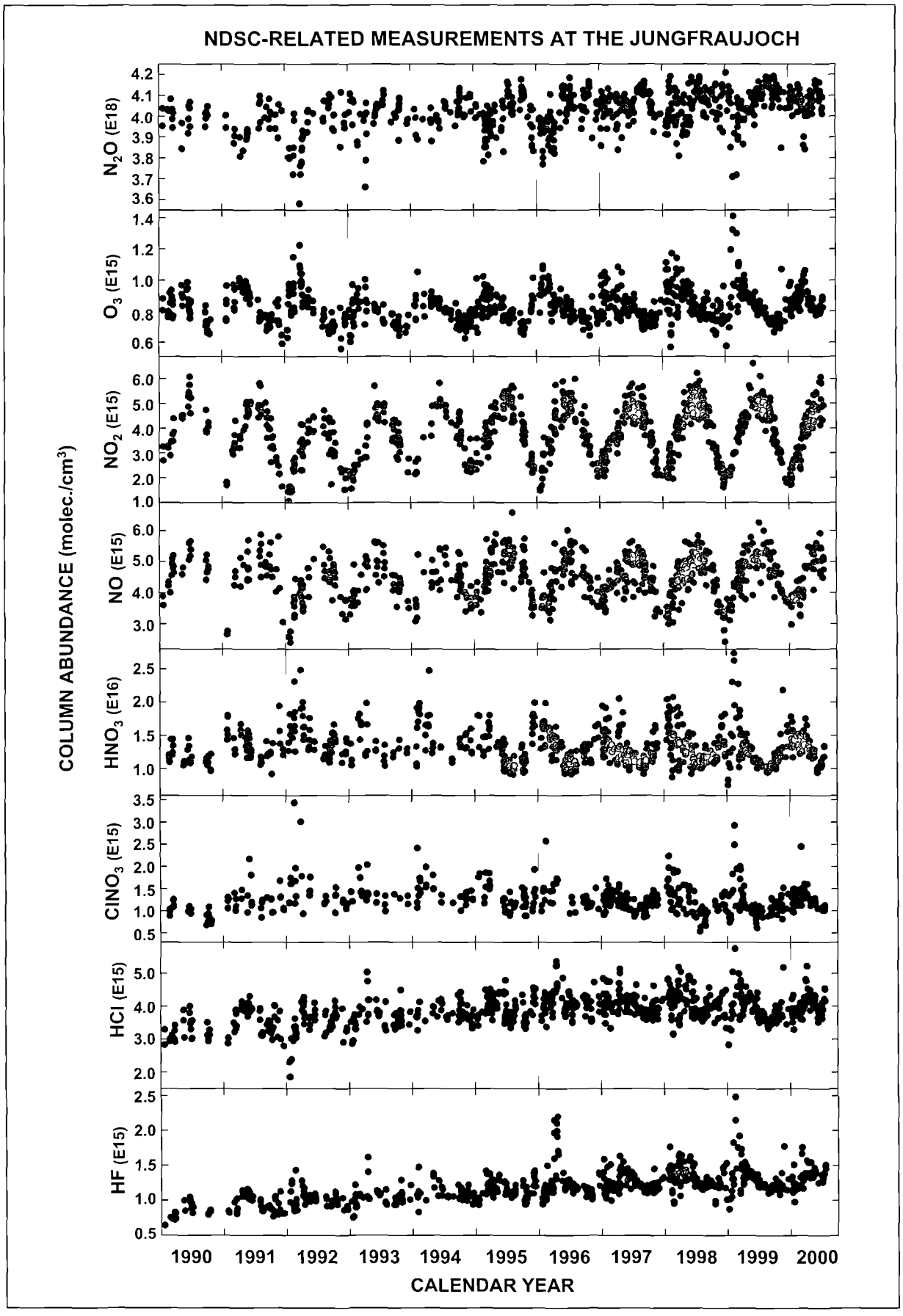

Figure 2.9 *Sample data of vertical column abundances of eight species recorded at the Jungfraujoch as part of the ULg contribution to NDSC-related activities on stratospheric changes. [Updated from Mahieu et al., 2000].*

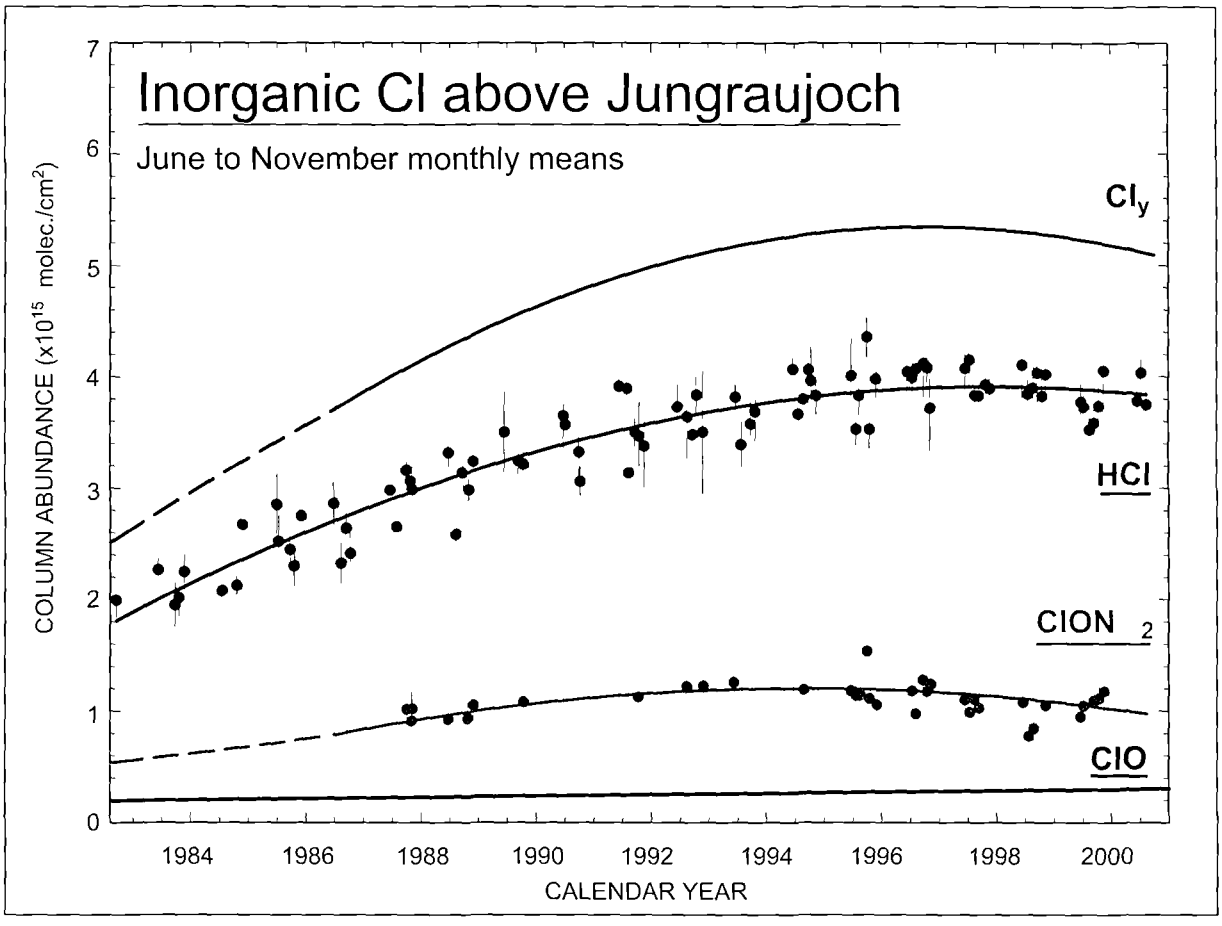

Figure 2.10 *The evolution of the burdens of HCl and $ClONO_2$ above the Jungfraujoch, based on June to November monthly mean vertical column abundances (to avoid large winter-spring variability). The reported Cl_y includes a ClO background load derived from model calculations. [Updated from Mahieu et al., 2000].*

Ny-Ålesund/Spitsbergen (79°N, 12°E, 10 m asl) since March 1992 [Notholt et al., 1997a, 1997b]. These data further show significant variability due to the influence of heterogeneous chemistry inside the polar vortex. This variability leads to great difficulties in assessing long-term trends during winter from such data sets. Nevertheless and despite the difficulties generally associated to monitoring activities in polar regions, good long-term measurements are starting to build up at the high-latitudes stations of the NDSC (see Box). This concerns in particular the active chlorine species ClO, measured by the microwave technique [Klein et al., 2000a], and OClO now measured on a quasi-routine basis by UV-visible spectrometers [Frieß et al., 1998; Otten et al., 1998].

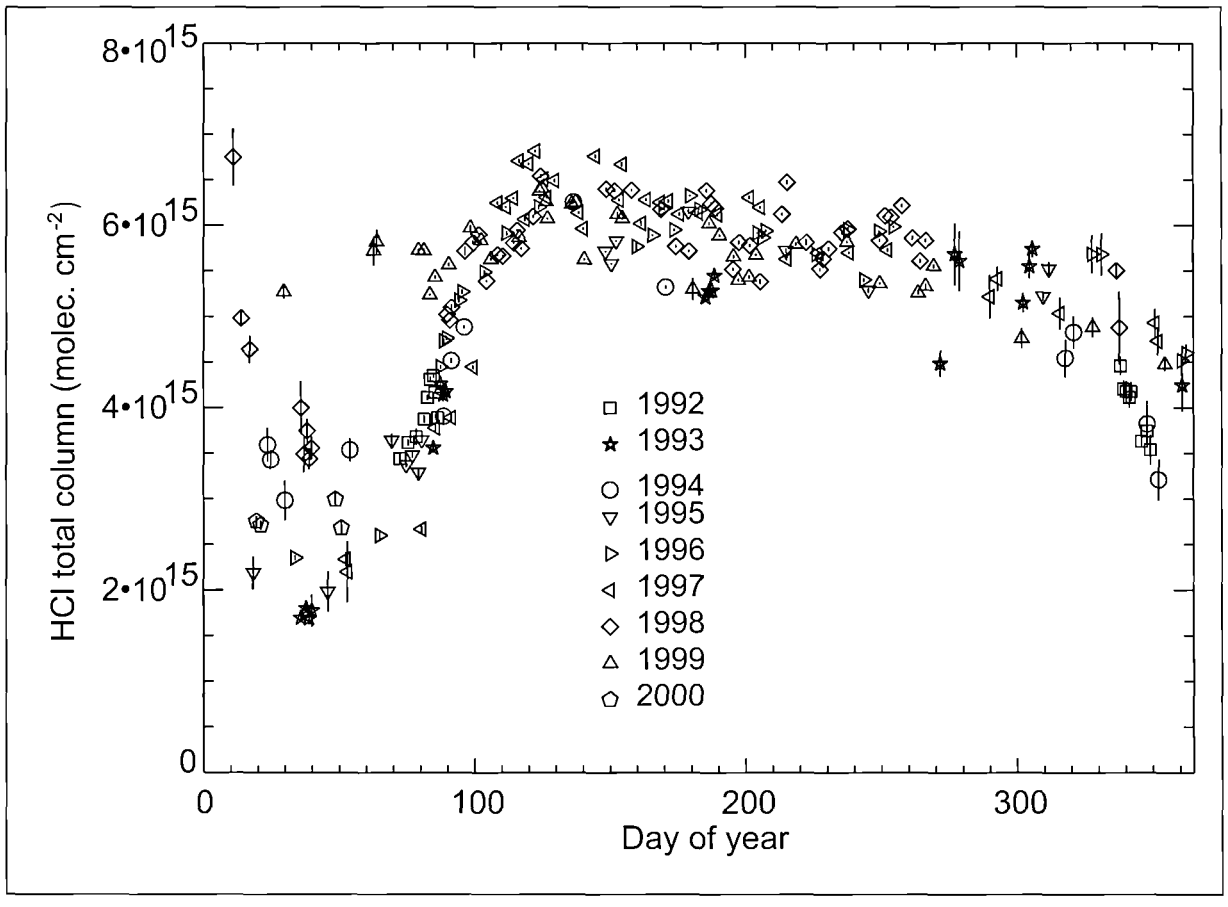

Figure 2.11 *Seasonal variation observed in HCl total columns above Ny-Ålesund, Spitsbergen (79°N, 12°E, 10 m asl) since March 1992 by FTIR spectrometry. [Updated from Notholt et al., 1997a].*

EUROPEAN CONTRIBUTION TO THE NDSC

After a decade of formal activities, the NDSC has reached routine and reliable operation of a series of specific instrument types (e.g., Dobson and Brewer, UV-Visible, FTIR, Lidar, Microwave, Ozone- and Aerosol sondes, spectral UV). Its dual goal of observing and understanding changes in the stratosphere from as many as five primary stations and over forty complementary sites has required rigorous quality control procedures based on regular instrument inter-comparisons and calibrations, as well as on validation activities of retrieval algorithms and multi-dimensional chemistry-transport models.

In terms of field observations, the European contribution to the NDSC has continued to increase, with active operations currently performed at three primary stations and at over 20 complementary sites (see Figure box 2.1). Related assimilation/modeling activities have also become more attractive and substantial, as data sets for an increasing number of atmospheric constituents extend over longer time periods and become available as validated products at the dedicated NDSC- Data Host Facility of NOAA (USA) and at NILU (Norway) (see NADIR web page for further information: <http://www.nilu.no/projects/nadir/>). A complete description of NDSC objectives, structure, operation, data archiving and related protocols and publications can be found at the home web page <http://ndsc.ncep.noaa.gov/>.

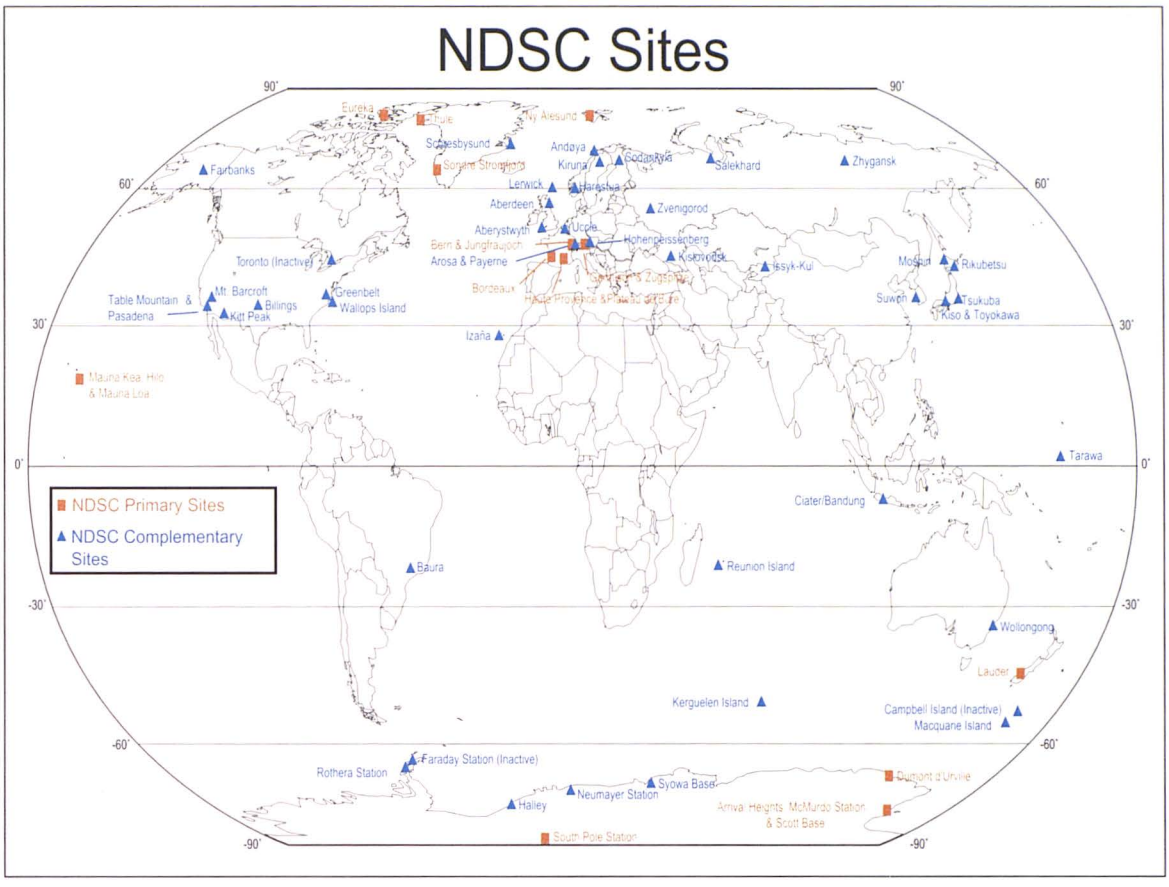

Figure box 2.1 *Map showing the global distribution of primary and complementary stations of the Network for the Detection of Stratospheric Change. Europe has a strong involvement in the NDSC, with operations being currently performed at 3 primary sites and over twenty complementary sites.*

Although it remains committed to monitoring changes in the stratosphere, with an emphasis on the long-term evolution of the ozone layer (decay, stabilisation, recovery,...), the NDSC has worked on ways to adapt progressively to new challenges arising from advances in scientific understanding of environmental problems and to scientifically justified implementations resulting from political developments. Among the latter are the amendments and adjustments to the Montreal Protocol and the more recent Kyoto Protocol (1997) seeking stabilisation of substances with large Greenhouse Warming Potentials that alter the radiative forcing of the climate system.

As part of its involvement in the NDSC, Europe has played an active role in developing or improving several important aspects of the techniques operated within the network. Most notably these have included the optimisation of new profiling techniques applied to FTIR observations and their scientific exploitation [Mellqvist et al., 2000], the development within the EMCOR project of new highly sensitive microwave techniques to measure stratospheric minor constituents [Gerber et al., 2000; Maier et al., 2001], and the improvement of the sensitivity and precision of the UV-visible DOAS technique for the measurement of key minor species, in particular BrO [Aliwell et al., 2001a].

2.3.2 Bromine species

In recent years considerable progress has been achieved in our understanding of the chemistry and budget of stratospheric bromine, in particular within two projects supported by the EU during the THESEO campaign: HALOMAX (Mid and high latitude stratospheric distribution of long and short lived HALOgen species during the MAXimum chlorine loading) and Stratospheric BrO.

The budget of inorganic bromine in the stratosphere (Br_y = BrO + $BrONO_2$ + HOBr + BrCl + HBr + ...) has been investigated by employing two methods: (a) the budget of organic source gas (Br_y^{org}) and (b) total bromine inferred from stratospheric BrO measurements using a modelled BrO/Br_y partitioning (Br_y^{in}) [Harder et al., 2000; Pfeilsticker et al., 2000a]. For early 1999 these studies revealed that (Br_y^{in}) has a mixing ratio of 1.5 pptv in air just above the local Arctic tropopause (approx. 9.5 km), whilst at 25 km in air of 5.6 year mean age it was estimated to be 18.4 (+1.8/–1.5) pptv from organic precursor measurements, and 21.5 (±3.0) pptv from BrO measurements and photochemical modelling, respectively [Pfeilsticker et al., 2000a].

Spectrometric BrO observations from balloons, together with measurements of the age of the probed air masses obtained through simultaneous measurements of long-lived source gases of known atmospheric trend, such as CO_2 or SF_6, provide new information on the trend in stratospheric bromine [Pfeilsticker, 2000]. Figure 2.12 displays the situation. As expected, the total stratospheric bromine inferred with the organic bromine method closely follows the measured trend of the tropospheric bromine-bearing sources gases, except for the Schauffler et al. [1998] data that is only a proxy for stratospheric bromine content. Total bromine inferred with the inorganic method also follows this trend, but it is 1-2 pptv larger, possibly because the organic bromine method does not account for a suspected influx of inorganic bromine into the stratosphere [Fitzenberger et al., 2000; Harder et al., 1998, 2000; Ko et al., 1997; Pfeilsticker et al., 2000a; Sturges et al., 2000]. The compilation thus provides evidence that the stratospheric bromine has increased from about 16-20 pptv (i.e. by about 25%) during the decade (1987-1996). Primarily this increase in stratospheric bromine is due to the increase in the atmospheric content of the halons H-1211 (by about 250%), H-1301 (by about 250%), H-2402 (by about 190%), and H-1202 (by about 200%) [Fraser et al., 1999].

Measurements of the surface concentrations of $CBrClF_2$, $CBrF_3$, $CBrF_2CBrF_2$ and CBr_2F_2 (respectively halons -1211, -1301, -2402, and -1202) have been made at the University of East Anglia (Norwich, UK) based on air from the CSIRO Cape Grim air archive [Fraser et al., 1999]. These analyses show that total bromine in halons has increased by a factor of 10 since the late 1970s and continues rise, largely because of the ongoing growth of halon-1211. Despite ceasing production of H-1211 and H-1301 in the developed world at the end of 1993 under provision of the Montreal Protocol, possible causes for the continued increase of halons are releases during the 1990s from the large halon "bank" that accumulated in developed countries during the 1980s and increased production of H-1211 in developing countries [WMO, 1999]. Halon increases over the next few years could delay the time of the currently expected total organic bromine maximum in the troposphere, and could cause the abundance of equivalent chlorine (see Section 2.3.3) to decline more slowly than predicted. It is therefore of great importance to pursue the monitoring of tropospheric and stratospheric bromine loadings during the upcoming decades in order to assess its impact on stratospheric ozone under conditions of reduced chlorine loading.

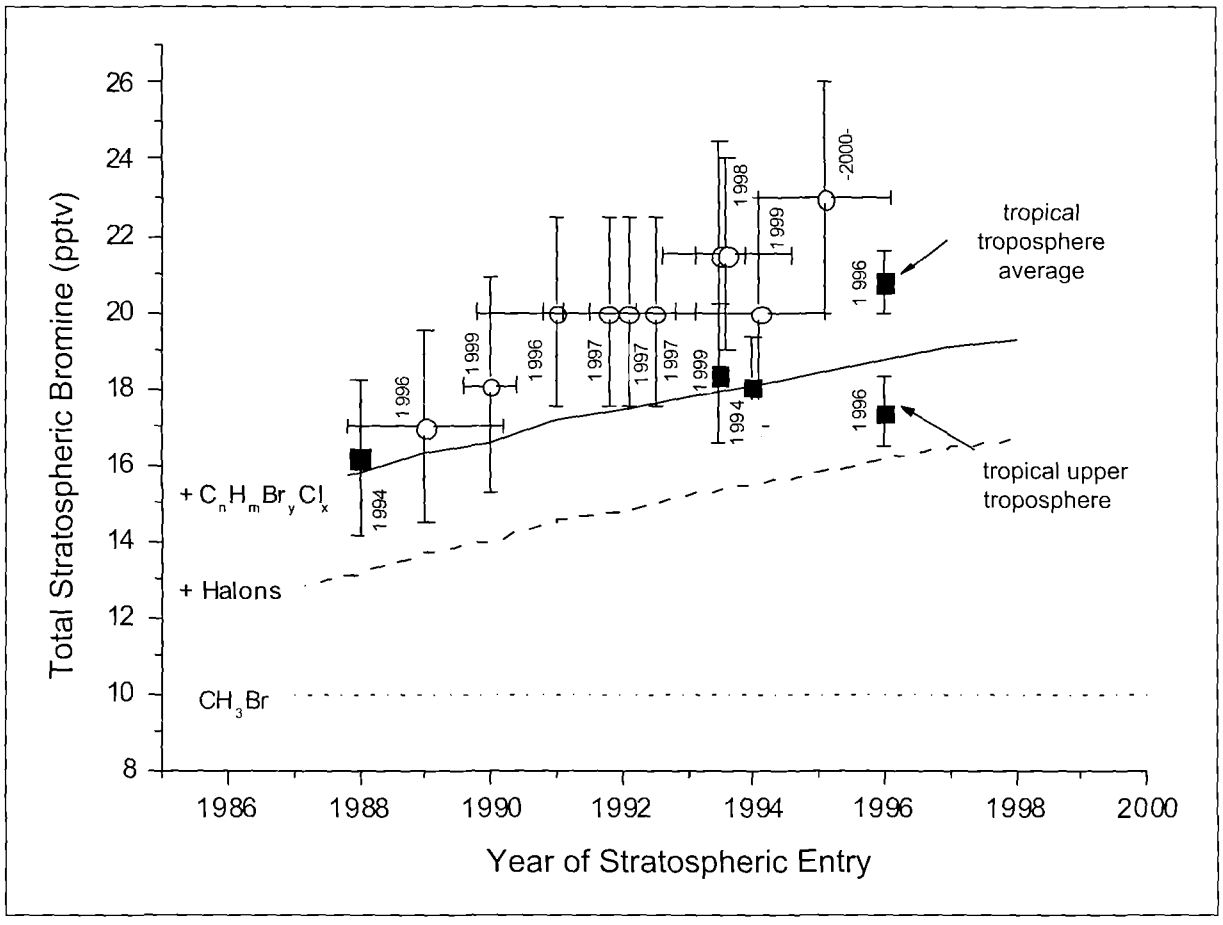

Figure 2.12 *A recent history of the total organic and inorganic stratospheric bromine inventory [updated from Pfeilsticker, 2000]. The dotted magenta line corresponds to a global averaged CH_3Br surface concentration of 10 pptv. The dashed blue line denotes the added trend of surface halon concentrations (H-1211, H-1301, H-2402, and H-1202). The solid blue line denotes the added tropospheric inventory of short-lived bromocarbons ($C_nH_mBr_yCl_x$) [Fraser et al., 1999]. The blue filled squares are measurements of total organic bromine in the upper troposphere and lower stratosphere by Wamsley et al. [1998] and Schauffler et al. [1998, 1999]. The open circles denote the total inorganic bromine inferred from stratospheric BrO measurements and photochemical calculations, accounting for the BrO/Br_y ratio [Harder et al., 1998, 2000; Pfeilsticker et al., 2000a]. The years when these measurements were made are given next to reported data.*

The capabilities of remote sensing instruments to monitor BrO from the ground [Richter et al., 1999], balloon, aircraft and space using UV-visible spectroscopy have been successfully assessed within the Stratospheric BrO project [Van Roozendael et al., 2000]. This will form the basis of the future observing system for long-term global monitoring of BrO (i.e. 60% of the available inorganic bromine during daytime). As an example, Figure 2.13 shows time series of BrO differential slant columns measured at six European stations of the Stratospheric BrO ground-based network from 1998 until mid-2000. These observations have been used to characterise and test against 3-D chemical transport simulations the short-term, seasonal and secular variations of BrO at various latitudes [Sinnhuber et al., 2000a, 2001].

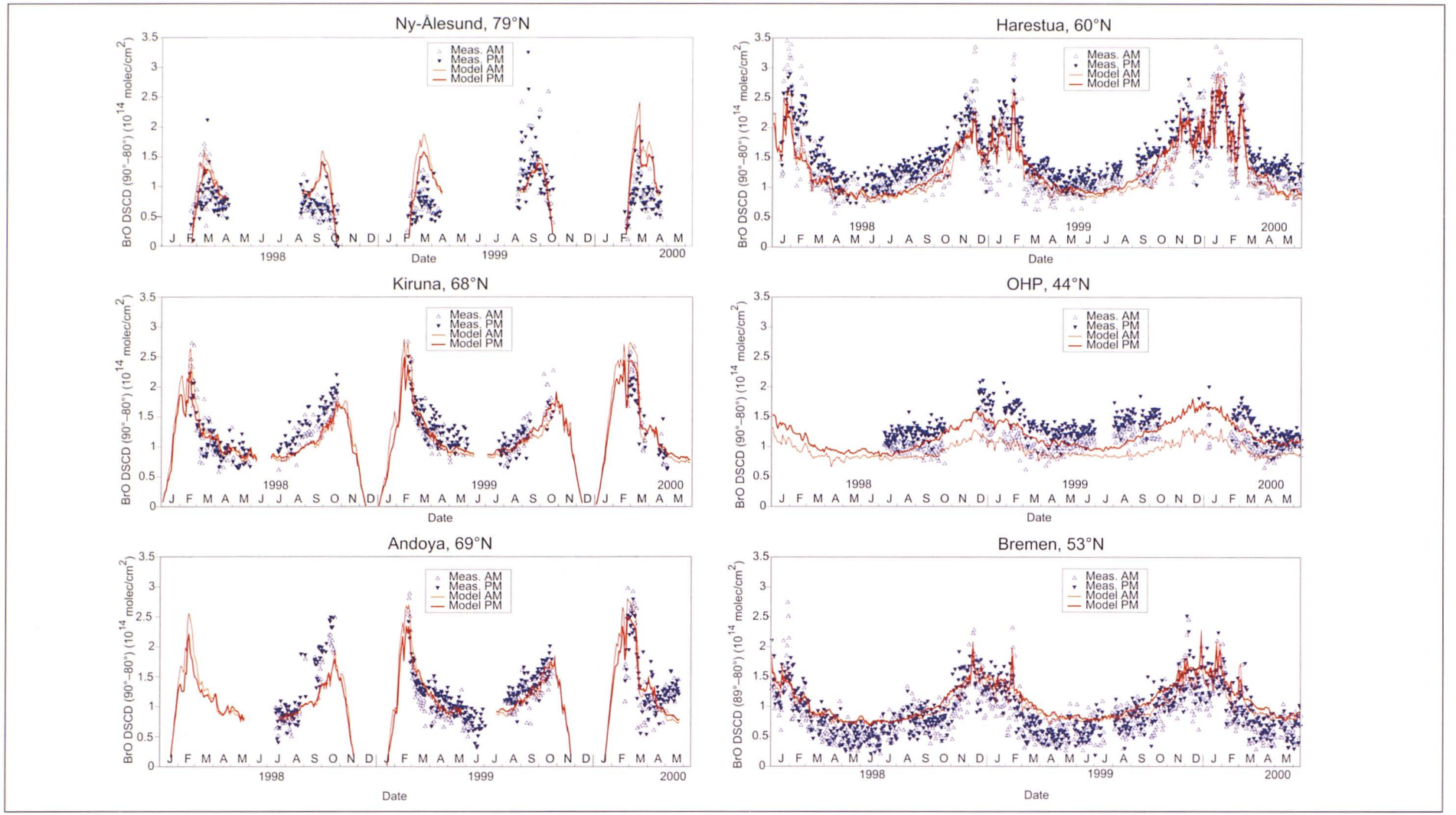

Figure 2.13 *BrO differential slant column between 90° and 80° SZA measured at six stations of the Stratospheric BrO network from 1998 until May 2000. AM and PM measurements (blue symbols) are compared to simulations from the SLIMCAT 3-D model (red lines). The grey shaded areas indicate periods when the sun did not reach solar zenith angles of 80°. Twilight BrO measurements exhibit a latitude-dependent seasonality mainly controlled by variations in stratospheric NO_2. [Sinnhuber et al., 2000a, 2001].*

2.3.3 Total Equivalent Chlorine

In order to estimate how the future abundance of stratospheric ozone will respond to simultaneous decreasing chlorine amounts and increasing bromine from halons, the trends for both Cl- and Br-containing species must be considered. This is true despite the comparatively low atmospheric concentrations of bromine, because on a per-atom basis, Br has a much larger catalytic efficiency at destroying ozone than chlorine. The relative impact of bromine compared to chlorine upon stratospheric ozone is characterized by the so-called α parameter [e.g. Solomon et al., 1992]. The values of α remain highly uncertain depending on a number of factors [Daniel et al., 1995], currently a mean value of 60 is being recommended by WMO [1999] when dealing with globally averaged ozone losses. The total equivalent chlorine is defined at a given time as the amount of tropospheric organic halogen that will become (at some future time) reactive inorganic halogen available to participate in the ozone depleting reactions. It can be estimated by weighting tropospheric mixing ratios of individual compounds according to their relative decomposition rates within different regions, and by accounting for the different catalytic efficiencies of chlorine and bromine using the α parameter. Calculations by Montzka et al. [1996] indicate that total equivalent chlorine peaked for polar regions in late 1993 and early 1994, and decreased afterwards at a rate of -18 ± 3 pptv per year. It should be noted that these numbers do not include the time lag between the troposphere and the stratosphere, which is a function of altitude, latitude and season. Continued increase of bromine loading due to emissions of anthropogenic halons could slow down this rate in the future.

2.4 TRENDS IN OTHER MINOR CONSTITUENTS

2.4.1 Water vapour and methane

Long-term changes of stratospheric water vapour are an important but still unknown parameter for the prediction of future changes of the ozone layer. Indeed, increasing water vapour concentrations could result in higher frequencies of polar stratospheric clouds and therefore delay the expected recovery of the ozone layer [WMO, 1999], especially if the build-up of greenhouse gases in the atmosphere results in a cooling of the stratosphere. Such a cooling could additionally be reinforced by the presence of increased water vapour amounts. These issues are further investigated in Chapter 5 of this report.

In the SPARC water vapour assessment [Kley et al., 2000], water vapour trends have been assessed. From a multi-decadal record of balloon launches over Boulder, Colorado, Oltmans and Hofmann [1995] and Oltmans et al. [2000] derived an increase of water vapour in the lower stratosphere exceeding 1% per year over the period 1980-2000. The observed increase is similar at all altitudes between 16 and 26 km and highly significant at all levels above 16 km. Using all published data sets, Rosenlof et al. [2000] assess a likely 1% per year increase of water vapour in the stratosphere since the middle 1950s (2 ppmv in all). Up to a half of this increase can be understood as arising from the increase in tropospheric methane since 1950 (0.55 ppmv), since photochemical oxidation of methane in the stratosphere produces approximately two molecules of water vapour per molecule of methane. The reason for the remainder of the reported increase in stratospheric water vapour remains unclear.

Up to now, the European *in situ* measurement record of H_2O, only available since the 1990s, cannot be used for a similar analysis. It is expected however that relevant data sets will become

sufficiently large within the coming years to follow the current changes. Unsuccessful attempts to identify a water vapour trend in the period 1992-2000 were recently reported by Schiller [1999] based on an analysis of available data sets of $2xCH_4+H_2O$ [Engel et al., 1996; Stowasser et al., 1999; Zöger et al., 1999a]. This quantity is expected to be less sensitive to regional dynamical changes than a single H_2O measurement. This approach will be pursued in the near future as new observations become available.

The temporal increase of methane has also been investigated by FTIR spectrometry at several ground-based locations, i.e. in Europe at the NDSC stations of Ny-Ålesund and Jungfraujoch. The observations at Ny-Ålesund are performed with the sun as a light source, except during the polar night (October-February) when the moon serves as a source. Data on total vertical column abundance of CH_4 above the Jungfraujoch have been gathered routinely since the mid-1980s, but similar "historic" measurements were also made in 1950/51; a consistent analysis of this ensemble indicates that the vertical column abundance of CH_4 increased from 1.68 to $2.28x10^{19}$ molec cm^{-2}, or 35%, over the last fifty years. However, since the mid-1980s the rate of CH_4 growth has slowed significantly, by over a factor of three (Figure 2.14), in line with findings from ground-level *in situ* investigations reported in Chapter 2 of WMO [1999].

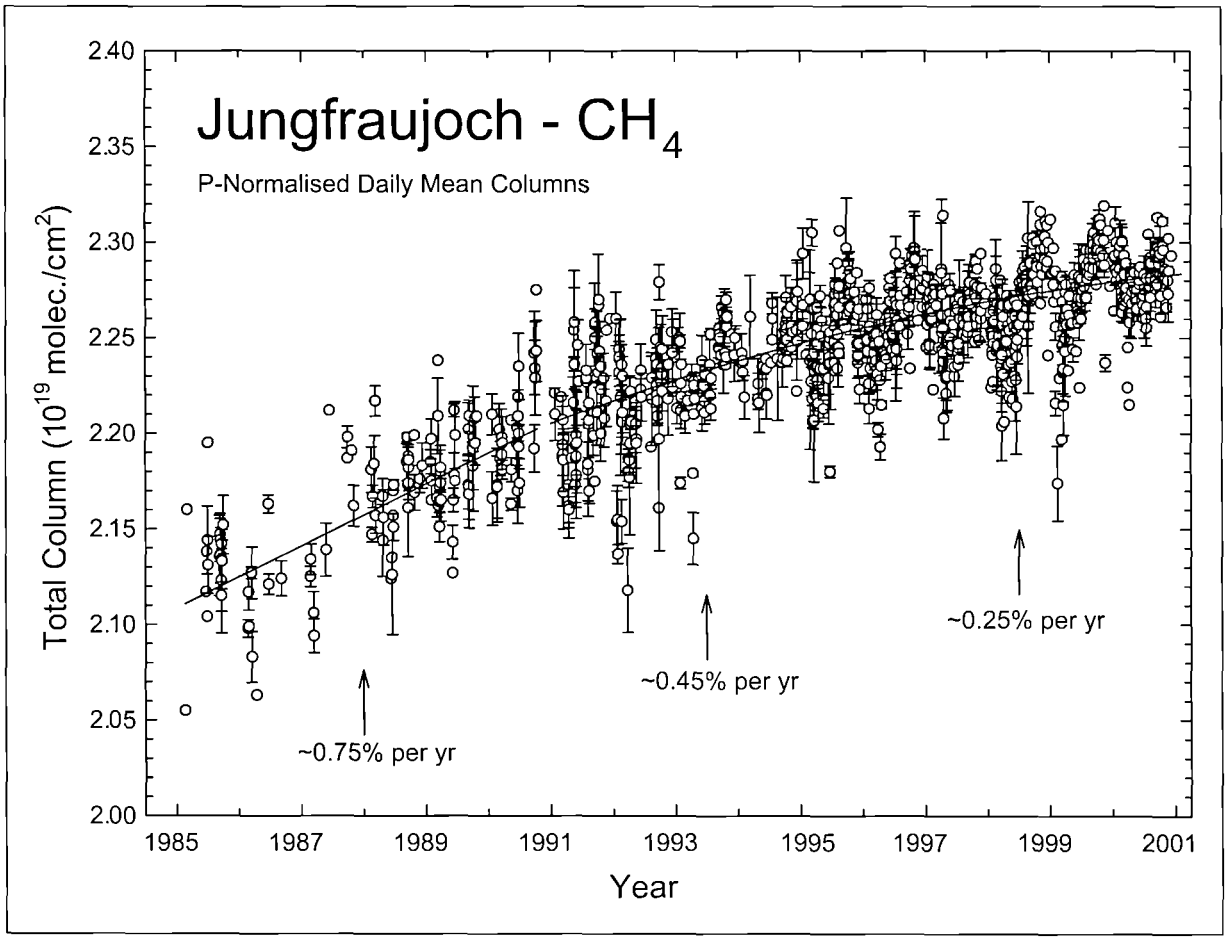

Figure 2.14 *Time series of daily mean vertical column abundances of CH_4 monitored above the Jungfraujoch from 1985 to 2000. Mean rates of increase during 1985-1990, in 1993 and in 1998 have been around 0.75, 0.45 and 0.25% per year. [Updated from Zander et al., 2000a].*

2.4.2 Nitrogen species

The importance of nitrogen oxides for stratospheric ozone concentrations has long been recognised. NO and NO_2 (NO_x) can destroy ozone catalytically, but they can also reduce ozone depletion caused by reactive chlorine and hydrogen compounds by converting these gases into unreactive reservoirs such as $ClONO_2$ and HNO_3. The source of stratospheric NO_2 and other nitrogen compounds (collectively known as NO_y) is N_2O released at the ground, then destroyed in the upper stratosphere by reaction with $O(^1D)$.

Surface N_2O concentrations measured *in situ* by the ALE/GAGE/AGAGE and the NOAA/CMDL networks increased globally at a rate of 2.8±0.3% per decade during the 1980s [Prinn et al., 1990; Elkins et al., 2000], slowing to nearly 2.0% per decade during the 1990s [WMO, 1999]. Since the mid 1980s, the vertical column abundance of N_2O has also been monitored by infrared absorption spectrometry at the Jungfraujoch, leading to a mean rate of increase equal to 3.3±0.2% per decade from 1985 to present (see bottom frame of Figure 2.15, an update of Zander et al. [1994, 2000a]). Reconciliation between these ground concentrations and the vertical column abundance trends of N_2O imply a raising of the tropopause above the Jungfraujoch by 150±50 m per decade [Zander et al., 2000b]. Similar tropopause height changes have been reported by Steinbrecht et al. [1998, 2000] and are probably related to the NAO (see Sections 2.6 and 2.5.3).

Recurrent long-term observations of NO_2 column abundances are part of the NDSC monitoring programme. They are made by UV-visible zenith-sky spectrographs and by FTIR spectrometers. A recently published analysis of slant columns of NO_2 observed at twilight by UV-Visible measurements between 1980 and 1998 at the primary NDSC station of Lauder (45.0°S, 169.7°E, 370 m asl) has identified a trend of about 5% per decade [Liley et al., 2000]. FTIR column measurements of NO_2 at the Jungfraujoch between 1985 and 2000 indicate a similar rate of increase of 6.5±2% per decade (see top frame of Figure 2.15, an update of Mahieu et al. [2000]). This is about twice the trend in tropospheric N_2O, which is the source of stratospheric NO_2. By means of a column photochemical model, Fish et al. [2000] have explored the sensitivity of NO_2 to the observed trends in stratospheric temperature, O_3 and H_2O. The resulting calculated trends in NO_2 are smaller than observed and no agreement can be found by varying the ozone or temperature trends. However, the calculated sensitivity of NO_2 to stratospheric aerosol loading is large, and a 20% per decade decrease in aerosol surface area leads to a reasonable agreement. The impact of the aerosol loading on the NO_2 abundance has been observed at various locations after the eruption of Mt Pinatubo in June 1991 [Goutail et al., 1994] and compared with model simulations [Van Roozendael et al., 1997]. At the Jungfraujoch observatory, the decrease and subsequent recovery of the NO_2 vertical column amount has been identified quantitatively, by exploiting the complementarity between the collocated UV-Vis and FTIR measurements [de Mazière et al., 1998]. In this same study, the long-term time series from both instruments have been validated mutually.

2.5 CHANGES IN STRATOSPHERIC CIRCULATION AND TEMPERATURE

The thermal structure of the stratosphere results from complex radiative and dynamical processes which are likely to change under the impact of anthropogenic forcing. The absorption of solar ultraviolet radiation and the emission of infrared radiation are affected by ozone depletion and the increase of greenhouse gases, respectively. Both effects are expected

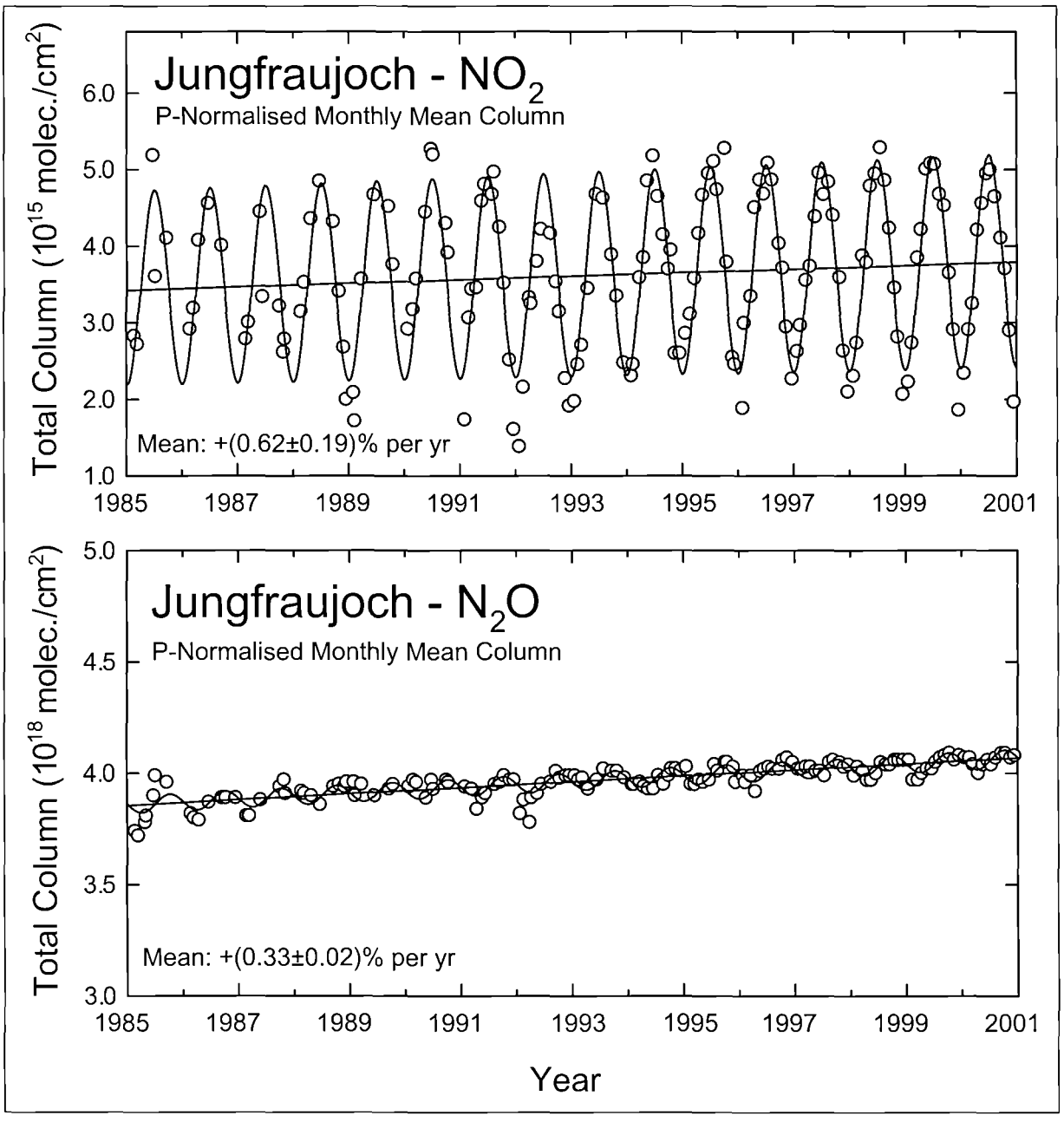

Figure 2.15 *Time series of monthly mean total vertical column abundances of NO_2 (top frame) [update from Mahieu et al., 2000] and N_2O (bottom frame) [update from Zander et al., 2000b] observed by FTIR spectrometry above the Jungfraujoch since 1985. Note the large reduction of the NO_2 column after the 1991 volcanic eruption of Mt Pinatubo [de Mazière et al., 1998] and the seasonal modulations affecting both compounds; also the different vertical scale units of both frames.*

to lead to a cooling of the stratosphere. Changes in the aerosol loading and in water vapour also affect the radiation budget. The transport of heat and mass by the general circulation can be affected by changes in radiatively-induced thermal gradients as well as by changes in the absorption of waves propagating up from the troposphere.

An extensive review of stratospheric temperature trends by Ramaswamy et al. [2001] came to the overall conclusion that the stratosphere has cooled considerably from the mid-1960s to the mid-1990s, most strikingly since 1979. It is generally agreed that a cooling trend is observed,

but it is still unclear how much can be attributed to anthropogenic forcing. The large dynamical variability in the northern polar region during late winter and spring makes reliable detection of trends in the Arctic winter difficult – either in the observations or in model simulations (see Chapter 5).

2.5.1 Natural Variability

The large inter-annual variability of the northern hemisphere in late winter and spring over polar latitudes is due to the occurrence of stratospheric warmings. The 30 hPa temperature deviations from the long-term monthly mean in January 1999 and January 2000 (Figure 2.16) impressively show the contrast between a warm and a cold winter. Since the essential mechanism for these warmings is the upward propagation of planetary waves from the troposphere and their interaction with the existing stratospheric flow, the occurrence and magnitude of this natural variability is influenced by variations in both the troposphere and the stratosphere. Factors influencing the state of the winter-time stratospheric circulation will now be described.

- During its easterly phase the ***Quasi-Biennial Oscillation*** (QBO) offers ideal conditions for the propagation of planetary wavenumber 1, leading to a strengthening of the Aleutian anticyclone and an amplification of poleward transport, thus to a more disturbed and warmer Arctic. During the westerly phase of the QBO the polar vortex tends to be colder and more stable. Gray et al. [2001] have shown that this sensitivity of the polar vortex to the equatorial wind direction is influenced by the phase of the QBO in the upper stratosphere and not just in the lower stratosphere, as previously assumed. Further details about the QBO may be found in the review by Baldwin et al. [2001].

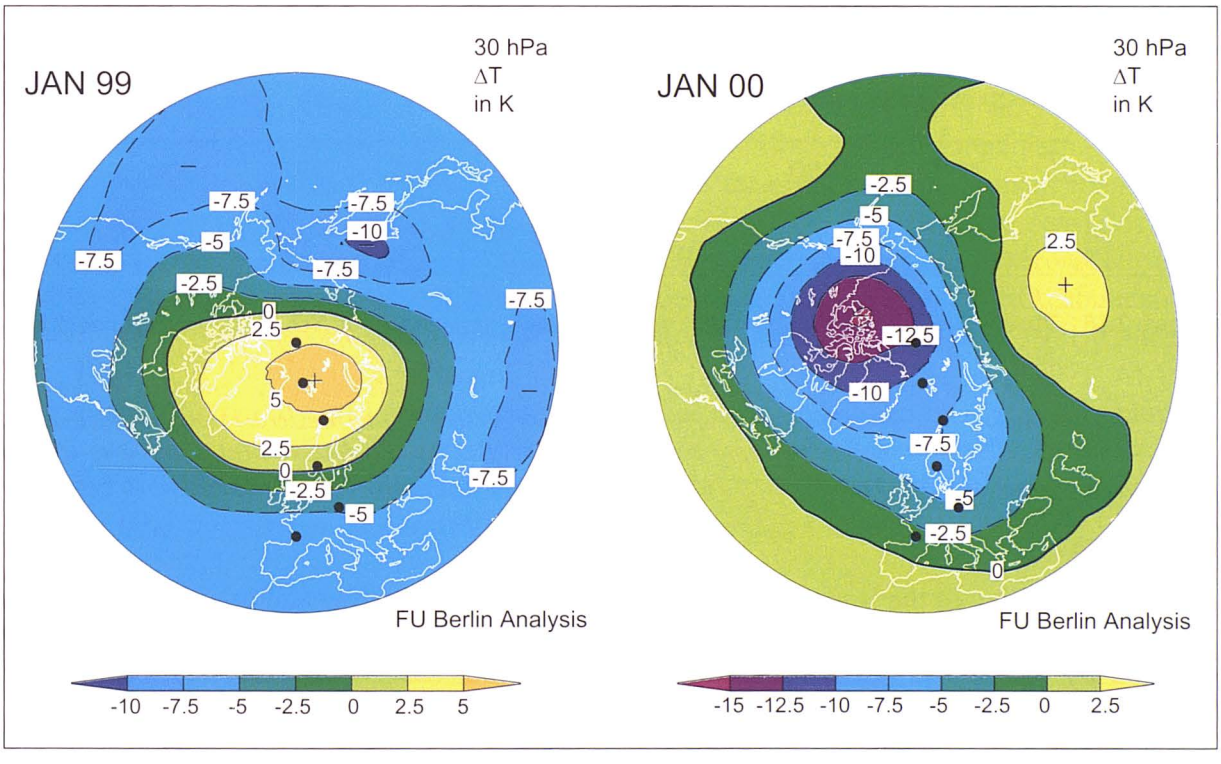

Figure 2.16 *30 hPa temperature deviations from the long-term means in January 1999 and 2000; dots indicate the North Pole and the nearest grid points to the observing stations Ny Ålesund, Kiruna, Oslo, Berlin, and Bordeaux (FU Berlin analyses).*

- The ***solar cycle*** modulates this expected connection between the QBO and the winter-time stratospheric circulation, weakening it during sunspot maximum. Labitzke and van Loon found statistically significant differences between the east and the west years of the QBO when they considered periods of sunspot minima, whereas during high solar activity the winters in the west phase of the QBO tend to be disturbed and are often connected with major mid-winter warmings [Labitzke and van Loon, 2000; van Loon and Labitzke, 2000]. This results in positive correlations between the 30 hPa geopotential heights and the 10.7 cm solar flux and in positive height differences between maxima and minima of the solar activity over the Arctic during the west phases of the QBO (Figure 2.17, lower panels). During the east phases (Figure 2.17, upper panels), negative correlations and negative height differences illustrate a more disturbed polar vortex in quiet sun periods, as expected from the QBO connection above.

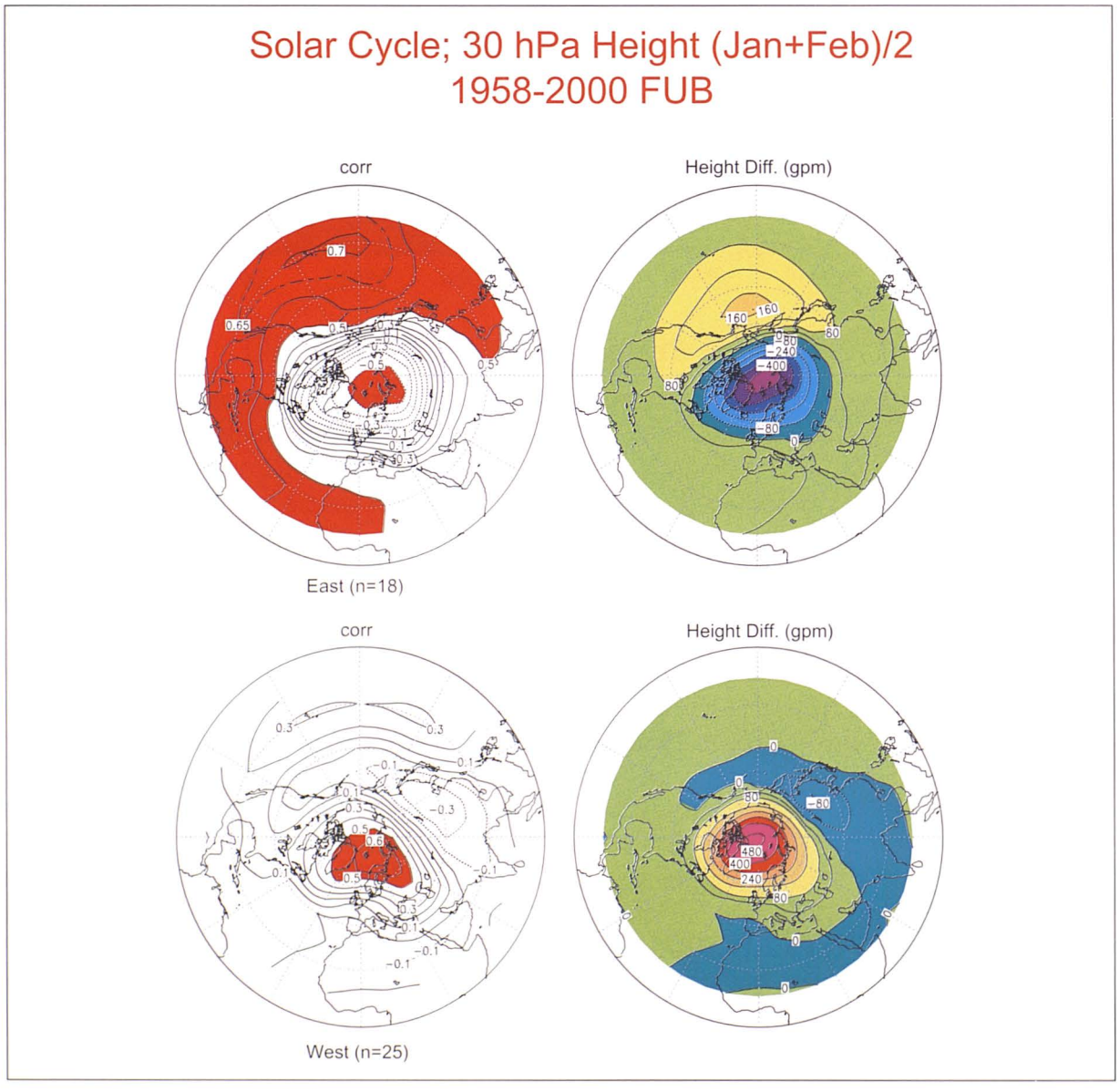

Figure 2.17 *Correlations between the 10.7 cm solar flux and mean 30 hPa heights in January/February for the period 1958-2000 (left, shaded are correlations above 0.5) and height differences between solar maxima and minima (right), grouped into the years in the east and west phase of the QBO. [Updated from Labitzke, 2001].*

- During a warm event of the ***El Niño/Southern Oscillation*** (ENSO), increased convection in the equatorial belt leads to a stronger upward motion of air and to a cooling of the tropopause and lower stratosphere in the tropics. Although this mainly results in dipole patterns over Indonesia and the central Pacific Ocean [Randel et al., 2000], there are also signals in the zonal averages of lower stratospheric temperatures over the tropics. The weaker temperature gradient to high latitudes causes weaker westerly winds, a stronger Aleutian anticyclone, and a weaker vortex. Warm ENSO events often result in major midwinter warmings and the associated mixing of air in the polar region with air from mid-latitudes while cold ENSO events are mostly connected with a cold and intense polar vortex [Labitzke and van Loon, 1999].

- The ***North Atlantic Oscillation/Arctic Oscillation*** (NAO/AO) modulates the stratospheric wintertime circulation; this is described further in Section 2.6.

- Finally, ***volcanic eruptions***, injecting gaseous material into the stratosphere which forms sulphate aerosols, additionally disturb the stratospheric temperature and circulation pattern for some time after the event. The aerosol loading after the three eruptions of Mt Agung (1963), El Chichon (1982), and Mt Pinatubo (1991) (see Section 2.8) caused a strong warming of the tropical stratosphere almost immediately (through direct absorption of long-wave radiation). Pawson et al. [1998] have shown that the observed negative trend in the 30 hPa annual mean temperatures over the northern hemisphere seems to have occurred in a stepwise manner following the volcanic eruptions of El Chichon and Mt Pinatubo.

2.5.2 Long-term changes

The trends in annual mean, zonally-averaged temperatures and geopotential heights in the northern hemisphere lower stratosphere for the period January 1965 to December 1999 are shown in Figure 2.18. The temperature trends are negative at all latitudes with maxima in the subtropics and in the polar region slightly above 50 hPa. Changes in the geopotential heights are positive in the lowermost stratosphere south of about 60°N, reflecting the vertically diminishing positive temperature trend in the troposphere, and negative to the north, becoming more so with height. This meridional distribution of height trends indicates a strengthening of the westerly winds at mid-latitudes.

Trends in the annual means in Figure 2.18 are the residual of different trend patterns in different months. In winter especially, the influence of natural variability leads to rather low statistical significance for stratospheric trends. Moreover, calculated trends strongly depend on the beginning and the end of the time series, e.g. the year 1979, when satellite data became available and when the ECMWF ERA-15 data begin, coincides with a maximum in solar activity. Figure 2.19 shows striking differences in the linear trends calculated for two different time periods of monthly mean 50 hPa temperatures – the level of the strongest cooling for the period 1965-1999 in Figure 2.18. The trends are negative for the longer period over the whole of the northern hemisphere, but weaker than for the shorter period, and strongest deviations are observed during the winter and spring months.

2.5.2.1 Winter and Spring

The longest data set available for stratospheric temperatures is that for the 30 hPa monthly mean temperatures over the North Pole from the FU Berlin analyses for the winters

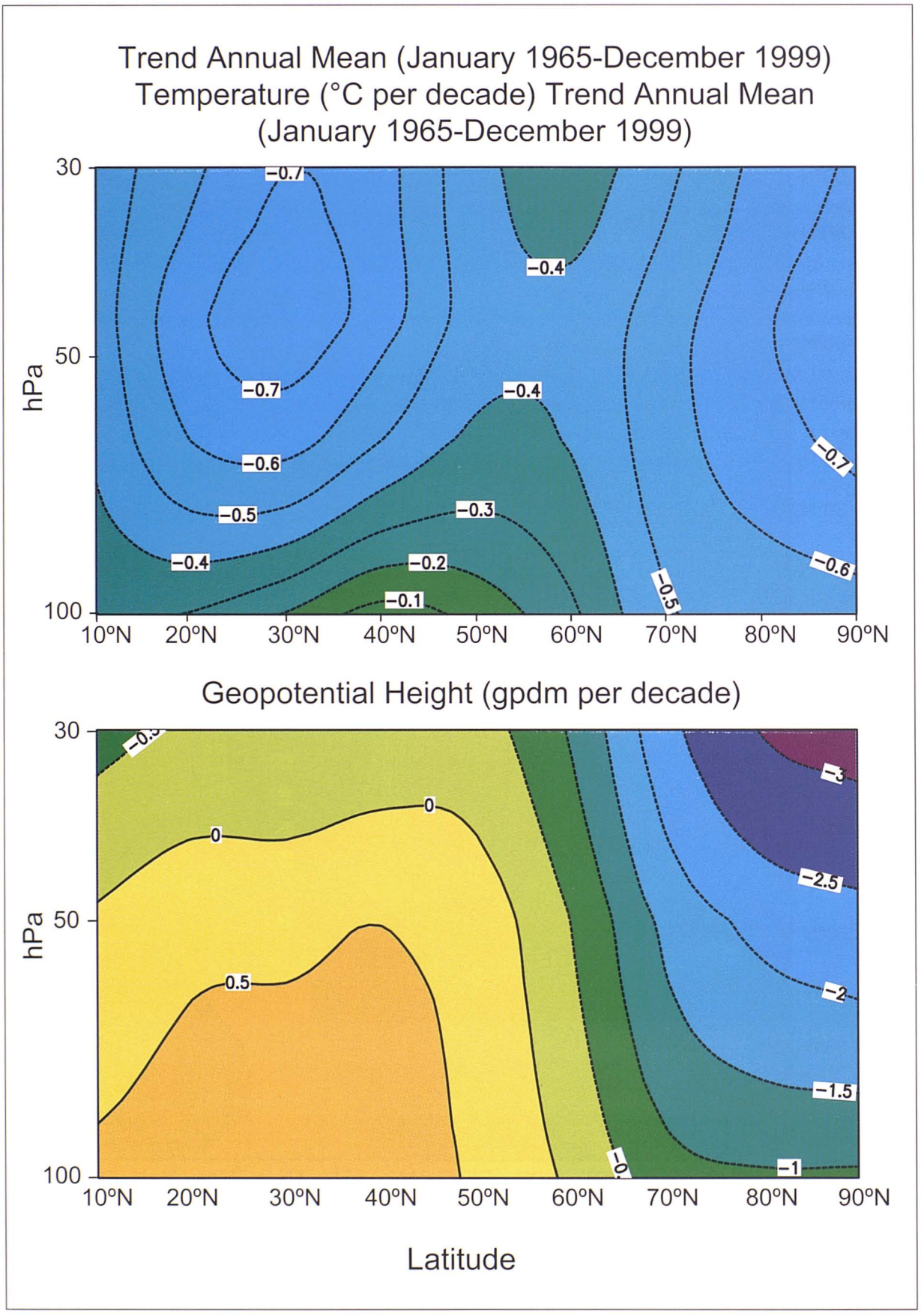

Figure 2.18 *Annual mean, zonally averaged trends of temperature (top) and of geopotential height in decametres (bottom) over the northern hemisphere between 100 and 30 hPa from FUB data for the period 1965-1999. [Updated from Labitzke and van Loon, 1994].*

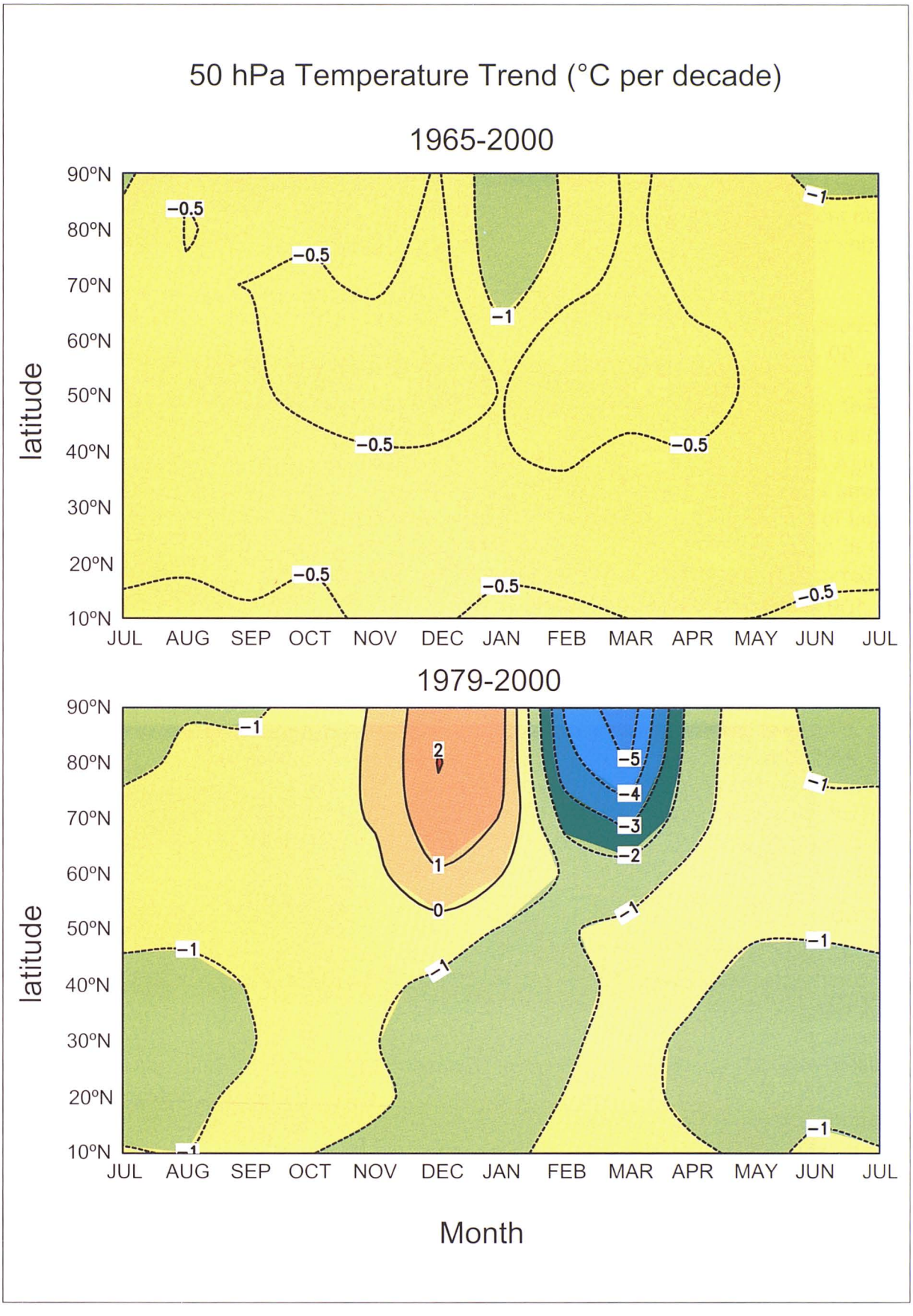

Figure 2.19 *Monthly mean, zonally averaged temperature trends at 50 hPa over the northern hemisphere for two different periods: 1965-2000 (top) and 1979-2000 (bottom) from FUB data. [Updated from Labitzke and van Loon, 1994].*

1955/56-1999/2000. These data exhibit a statistically significant linear trend only in November: –1.2 K per decade [Labitzke and Naujokat, 2000]. The winter months December, January, and February show slightly negative but not significant trends, and in March and April almost no trend at all is discernible.

A closer look at the monthly mean temperatures of forty-five winters reveals that in early winter a clear change in temperature and circulation took place. In November/December, Canadian warmings were frequently observed in the years until 1981/82, but have been almost absent for the last eighteen winters. This points to changes in tropospheric conditions, since the Canadian warmings are connected with intensification of the Aleutian stratospheric high/tropospheric low. While almost all Novembers have been cold in the past eighteen years, December has been more variable: very cold conditions were observed in some years, but also two major warmings took place (1987 and 1998), a feature not observed in the thirty-two years from 1952-1985. This is reflected in the positive trends for December for the period 1979-2000 in Figure 2.19. During the latter period six major warmings took place in January and eight in February, compared with one in January and three in February from 1986 onwards. Indeed, there was a period of seven winters from 1991/92-1997/98 without major warmings. A possible explanation for this is that the QBO was in a westerly phase during the four winters from 1993-1996, a sequence not previously experienced. In addition, solar activity was low during these winters.

Late winter/spring is an important time since a long-lasting cold vortex favours ozone destruction, while earlier break-ups of the vortex are connected with transport of ozone into the polar region. Figure 2.20 shows the 30 hPa monthly mean temperatures for March at the North Pole from 1956-2000. Linear trends have been calculated for three different periods: for the complete series the trend is zero, from 1956-1979 it is positive (and significant), and it is strongly negative (again significant) from 1979-2000.

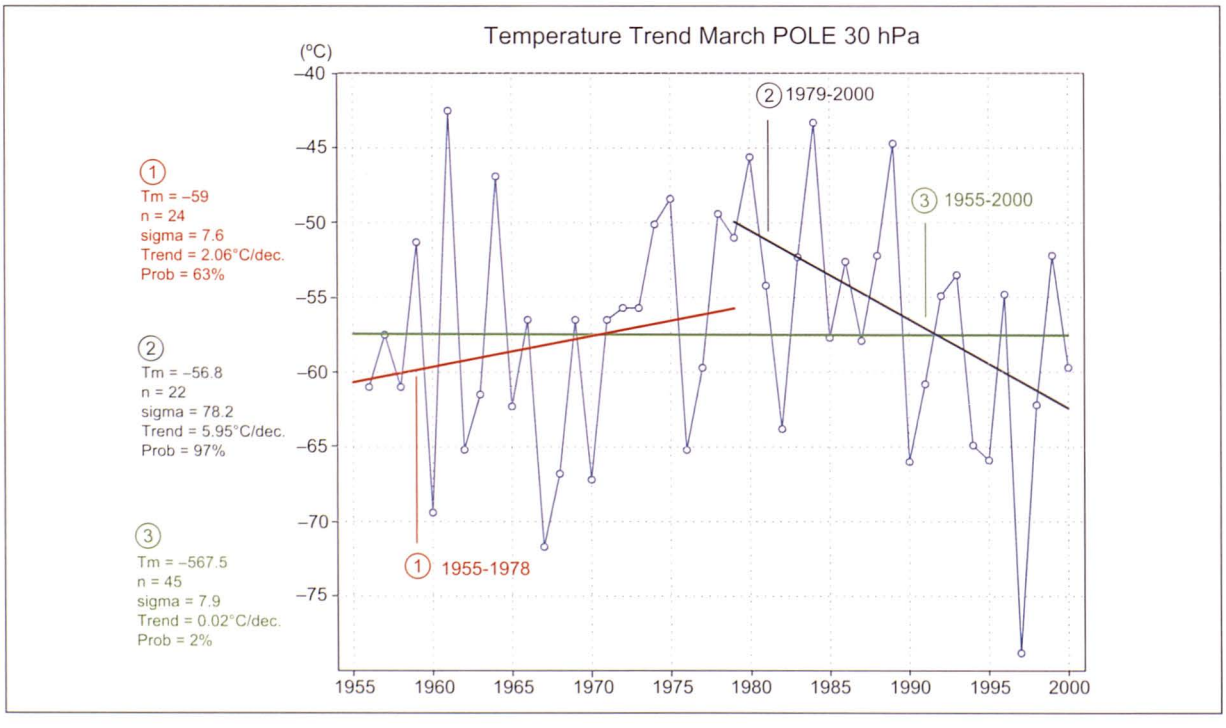

Figure 2.20 *Time series of 30 hPa monthly mean temperatures at the North Pole in March, 1956-2000 from FU Berlin data; linear trends have been computed for three different periods. [Updated from Labitzke and van Loon, 1999].*

Zonally and monthly averaged data possibly obscure the occurrence of extremely cold regions which are often associated with amplified planetary waves. The inspection of daily data revealed that the minimum temperatures reached on any day at any location of the northern hemisphere show a negative trend, at least until the winter 1996/97 [Pawson and Naujokat, 1997]. During the three winters of the middle 1990s extremely cold periods of long duration occurred and the coldness persisted into the late winter [Pawson and Naujokat, 1999]. The indicated cooling trend there was interrupted by the two warm winters 1997/98 and 1998/99, but continued by the winter 1999/2000 which was one of the coldest on record since the Berlin northern hemispheric temperature analyses began in 1964/65. Figure 2.21 shows the number of days for each winter season on which the minimum temperature was below the thresholds for the formation of Type 1 Polar Stratospheric Clouds (NAT PSC). In the lower part of Figure 2.21, the area of possible PSC formation over the northern hemisphere is shown, integrated for each winter. The linear trends reported before [Pawson and Naujokat, 1997] are slightly reduced when adding the recent years to the record, but still persist.

2.5.2.2 Summer and Autumn

The relatively undisturbed stratosphere in summer and autumn, when the predominantly easterly winds prevent the upward propagation of planetary waves from the troposphere, is

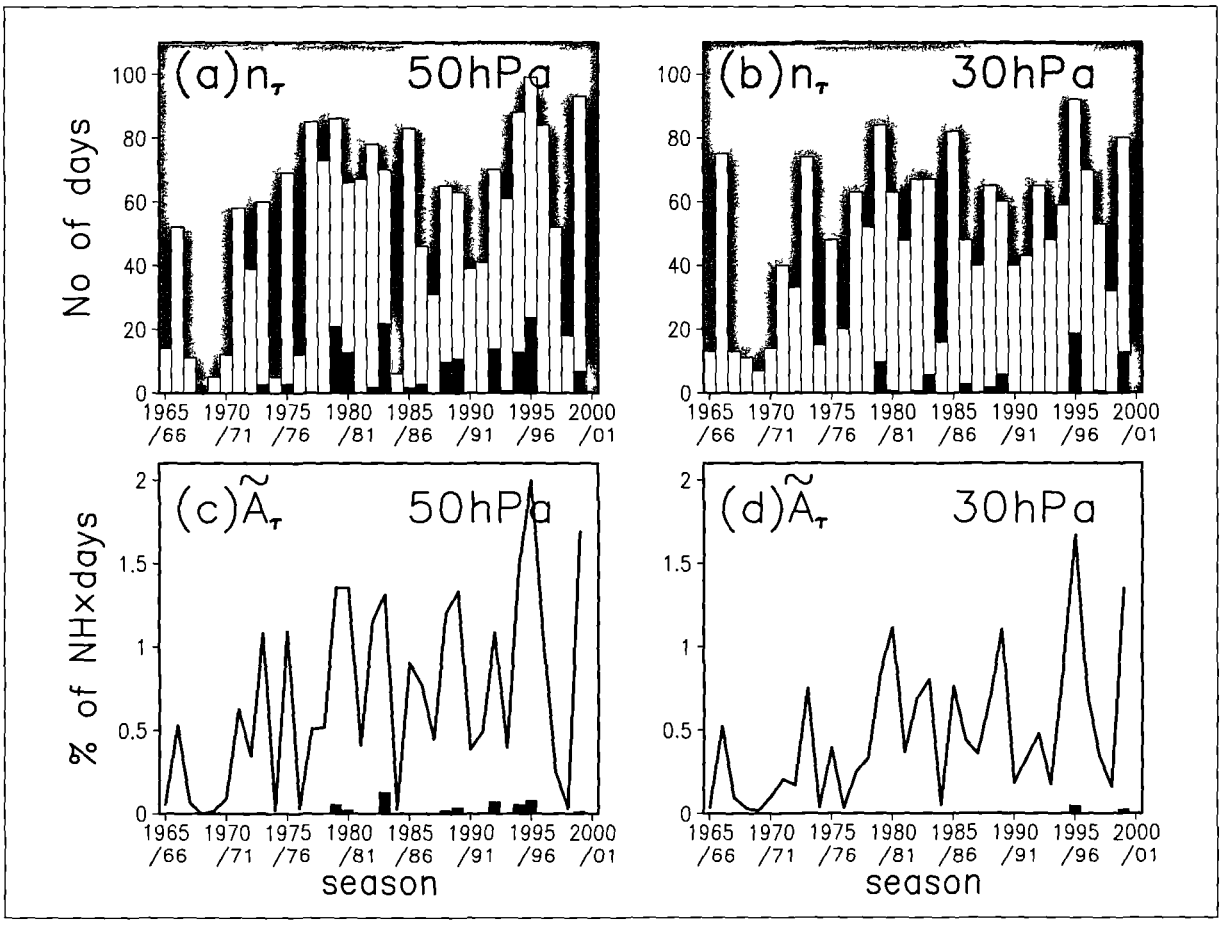

Figure 2.21 *Number of days (a, b) with minimum temperatures below the PSC thresholds for NAT and ice at 50 and 30 hPa and the integral of the areas of possible PSC formation (c, d) over the winter at 50 and 30 hPa for the winters 1965/66-1999/2000 from FU Berlin analyses. [Updated from Pawson and Naujokat, 1999].*

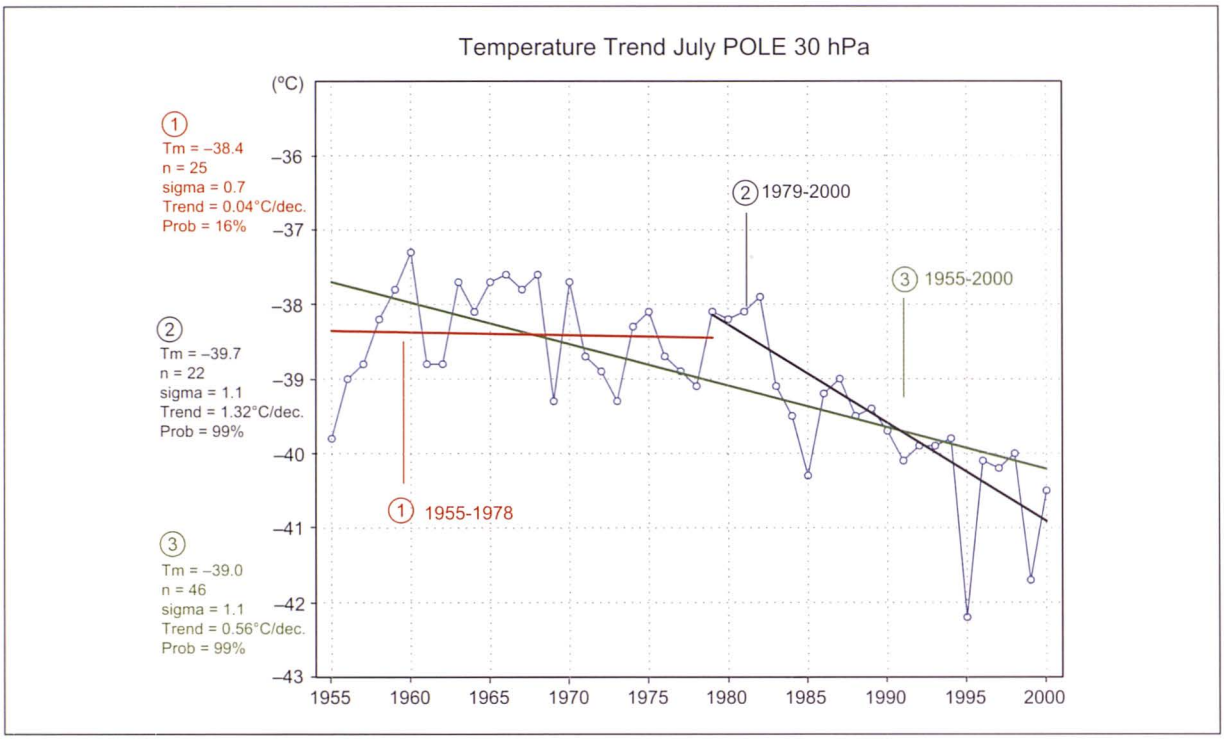

Figure 2.22 *Same as Figure 2.20, but for July.*

better suited to trend detection. Considering again the longest available period from 1955-2000, the 30 hPa monthly mean temperatures at the North Pole for July (Figure 2.22) shows a statistically significant negative trend of about 0.5 K per decade. The linear trend calculations for the two sub-periods 1955-1979 and 1979-2000 show more cooling in the latter period, thus suggesting that at least part of the observed strong cooling in the Arctic winter since 1979 might be attributed to a realistic trend in spite of the natural variability.

Figure 2.23 shows the northern hemispheric distribution of temperature trends per decade at 50 hPa in summer (average of June and July) for the period 1964-2000. The negative trends in this map are significant on the 99% level and are quite robust against different data periods.

2.5.3 Changes in the lowermost stratosphere

Changes to the circulation of the main part of the stratosphere affect the Brewer-Dobson circulation and the re-distribution of ozone around the planet, thus having a first-order influence on ozone. However, the dynamics of the troposphere also has a direct influence on the lowermost part of the stratosphere since short-wavelength Rossby waves can propagate into this region. In recent years it has become clear that mixing of subtropical, ozone-poor air into the mid-latitude lower stratosphere acts to reduce the ozone concentration there [O'Connor et al., 1999; Orsolini et al., 1995a; Vaughan and Timmis, 1998] and that this mixing is controlled by Rossby-wave breaking [Peters and Waugh, 1996]. There is some evidence that the frequency of Rossby wave-breaking events is increasing [Hood et al., 1999] and that layers of ozone-poor air in the lower stratosphere have become more common [Reid et al., 2000], although this may be another manifestation of the North Atlantic Oscillation (see Section 2.6). Indeed, Hudson and Frolov [2000] analysed trends in TOMS total ozone according to the

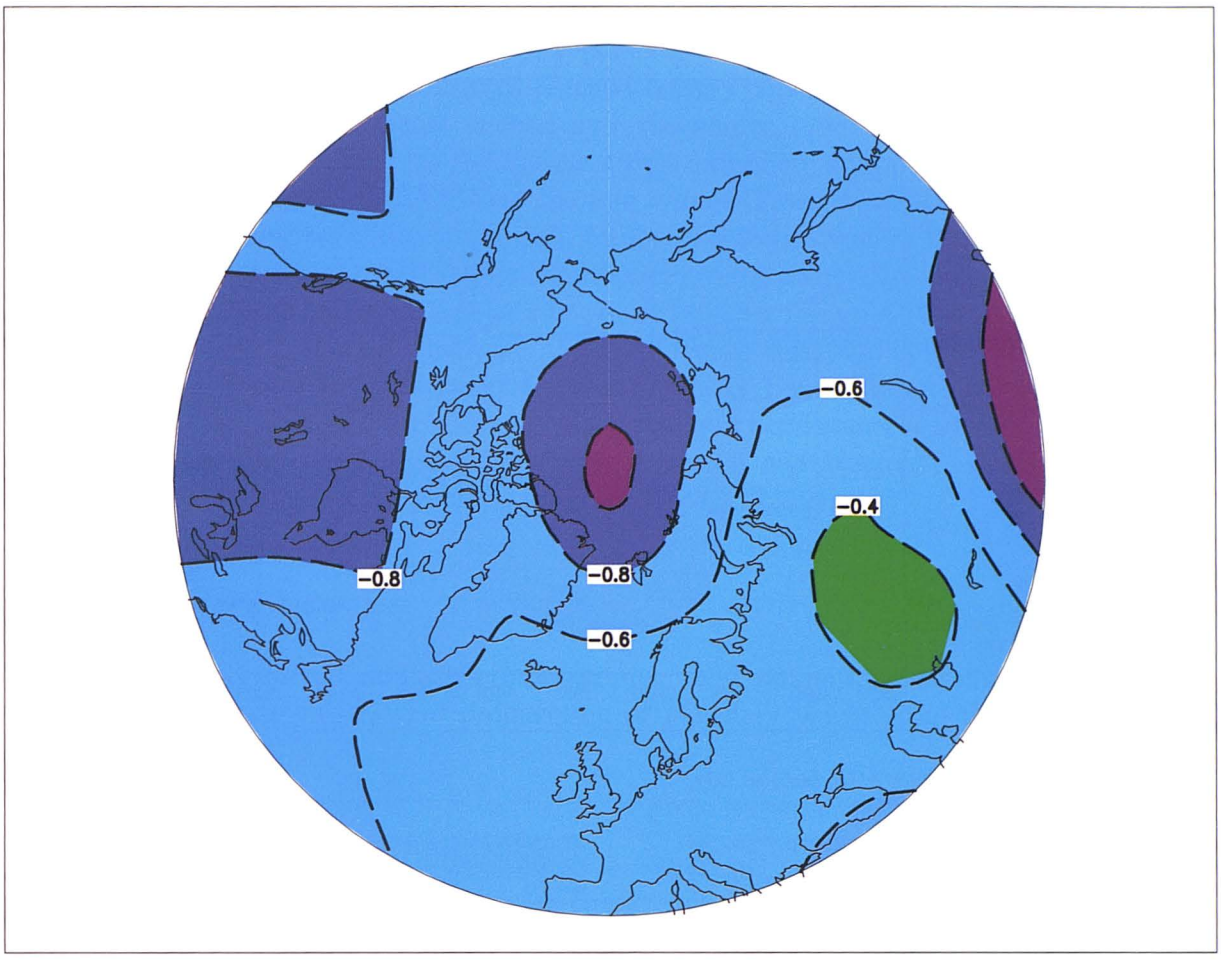

Figure 2.23 *Linear trend of 50 hPa monthly mean temperatures in June/July (K per decade) over the northern hemisphere for the period 1964-2000 from FUB data.*

meteorological regime of each measurement (tropical, mid-latitude and polar), and found no trend at all in total ozone within each regime. Their conclusion was that ozone changes in the northern mid-latitudes are caused by the systematic northward movement of the polar and sub-tropical jetstreams.

A 30-year data record (1967-1997) of vertical temperature and ozone profiles measured at the Meteorological Observatory Hohenpeissenberg (47.8°N, 11.0°E) was analysed with respect to trends [Steinbrecht et al., 1998]. They found that the tropopause height rose 150±70 m per decade over the period. This height shift is correlated with an observed warming of the troposphere, for example, 0.7±0.3 K per decade at 5 km altitude. Based on the well known anticorrelation between tropopause height and ozone column it was speculated that the increase in tropopause height could contribute approximately one third of the mid-latitude ozone reduction. This result however could be related to the North Atlantic Oscillation (see below).

2.5.4 Changes to the Arctic polar vortex

The Arctic polar vortex usually forms in November-December and breaks up in March-April. There are, however, large differences between individual winters in vortex duration, coldness and strength. Figure 2.24 presents the break-up dates of Arctic polar vortices and average vortex

strengths in the 1980s and 1990s, derived from ECMWF analyses using the method of Nash et al. [1996]. It is obvious that vortices in the 1990s have persisted longer than in the 1980s and also the isolation from mid latitudes has increased. The change of vortex persistence has been 3-4 weeks during the last two decades. Similar results have been reported from other studies using NCEP re-analysis data [Waugh et al., 1999]. Zhou et al. [2000], who studied vortex persistence at

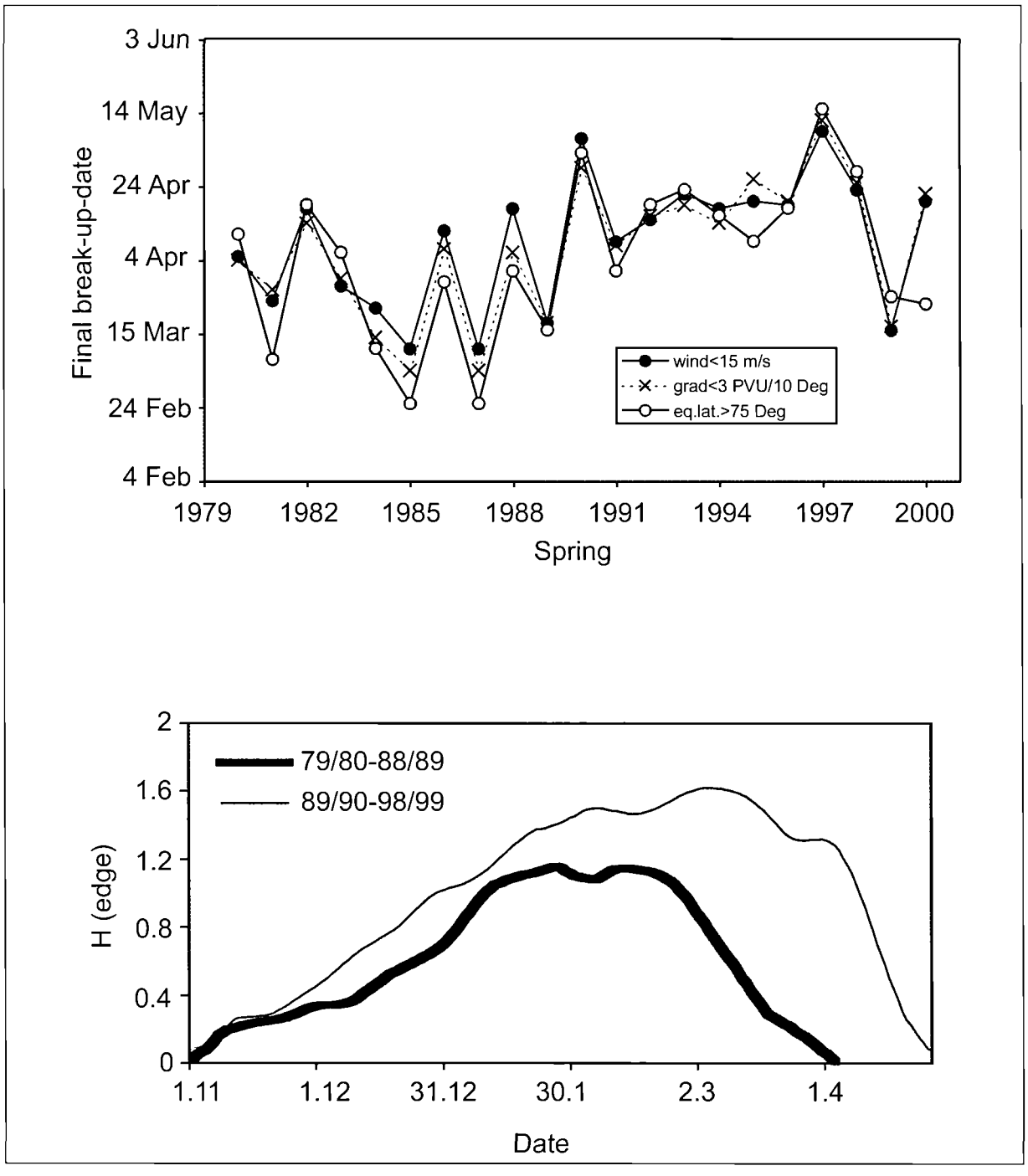

Figure 2.24 *Top panel: Vortex break-up dates at 475 K for twenty-one winters from 1979/80 to 1999/2000, determined from threshold values of three different parameters: maximum wind speed, maximum PV gradient with respect to equivalent latitude, and vortex area measured in terms of equivalent latitude [updated from Kyrö et al., 2000]. Bottom panel: Average vortex strength in the 1980s and 1990s defined as the mean PV gradient with respect to equivalent latitude at 475 K. [Updated from Kyrö et al., 2000].*

various isentropes from 400-650 K, also pointed out that the persistence has been greatest at altitudes where springtime Arctic ozone depletion is largest. However, this relationship is more clear in the southern hemisphere than in the northern hemisphere, where various dynamical influences may play an important role. Waugh et al. [1999] showed that the vortex persistence is closely linked to the February and March (but not January) polar temperatures at 50 hPa and the 100 hPa eddy heat flux between 45 and 75°N two months prior to the vortex break-up. However, the extremely long-lived vortices of the 1990s are not accompanied by similar extremes in heat fluxes. Coy et al. [1997] and Zhou et al. [2000] also suggested that the wave activity responsible for the final breakdown of the vortex has been weakening in the 1990s.

2.6 NORTH ATLANTIC OSCILLATION/ARCTIC OSCILLATION (NAO/AO)

Over the last five years considerable attention has been paid to the so-called NAO and AO and their relation to long-term changes in the stratosphere. The NAO index is defined by meteorologists as the surface pressure difference between Ponta Delgada (Azores) and Stykkisholmur (Iceland) [Hurrell, 1995]. Its signature appears in many meteorological and oceanic parameters in the North Atlantic and European regions, including the troposphere-stratosphere system [Appenzeller et al., 2000; Perlwitz and Graf, 1995], as indicated in Figure 2.25. The AO is a related phenomenon, best understood as the surface signature of modulation in the strength of the stratospheric polar vortex [Thompson and Wallace, 1998]. The AO is defined as the leading empirical orthogonal function of the northern hemisphere winter-time sea-level pressure field [Thompson and Wallace, 1998] and is correlated with the NAO. These climatic indices exhibit variability on time scales longer than most ozone records (Figure 2.26).

At present, the physical causes of the NAO and AO are unknown. Numerical simulations of the NAO show that an atmosphere-ocean interaction is indispensable for reproducing the climatic oscillation [Selten et al., 1999], but where the initial perturbations stem from remains unidentified, although there are suggestions that they come from the atmosphere [Marshall et al., 1997]. The response of the oceanic circulation to wind-stress anomalies appears to be essential. Another troposphere-ocean interaction is suggested by Mysak and Venegas [1998]: the feedback loop between polar ice coverage and surface winds. The AO extends from the surface up into the stratosphere and is strongly related to the strength of the polar vortex [Perlwitz and Graf, 1995; Thompson and Wallace, 2001]. Also, the apparent downward propagation of the AO signal from the stratosphere into the troposphere [Baldwin and Dunkerton, 1999] may indicate that the stratosphere has a significant influence on the tropospheric circulation. Gillett et al. [2001] found a significant shift in the AO distribution between 1958-1997 and 1978-1997 corresponding to a stronger polar vortex.

Perlwitz et al. [2000] have examined the response of the AO in a climate-change GCM experiment. They show that under increased greenhouse gas forcing the response is very similar to the AO mode of variability. They emphasise that a correct representation of the AO mode of variability, including a good representation of the stratosphere, is very important to correctly represent the atmospheric response to stratospheric aerosol, stratospheric ozone loss, changes in solar activity, and increased greenhouse gas forcing (as also has been indicated by the GCM studies of Shindell et al. [1999]).

Clearly, incomplete understanding of the NAO/AO makes climate forecasts difficult. Whether the present trend in the NAO is unique compared to historic behaviour or not is a moot point.

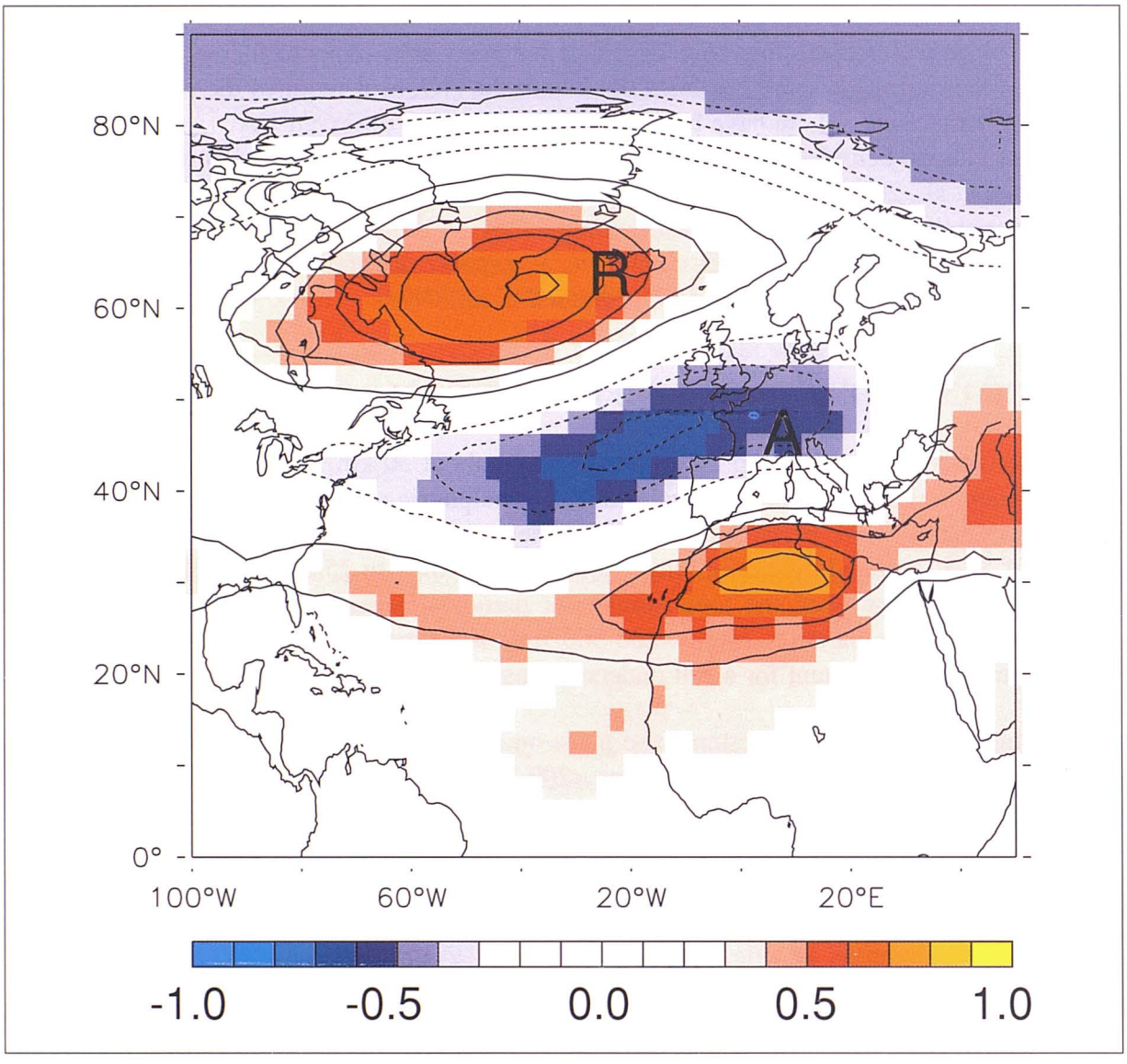

Figure 2.25 *Cross correlation map (in colours) between winter mean (December-March) tropopause pressure and NAO index both derived from NCEP reanalysis data for the period 1958 to 1998. Only correlation coefficients above/below ±0.3 are shown. Contours indicate tropopause pressure variation (in hPa) associated with +1σ in NAO index, (A) location of Arosa and (R) location of Reykjavik. [Appenzeller et al., 2000.]*

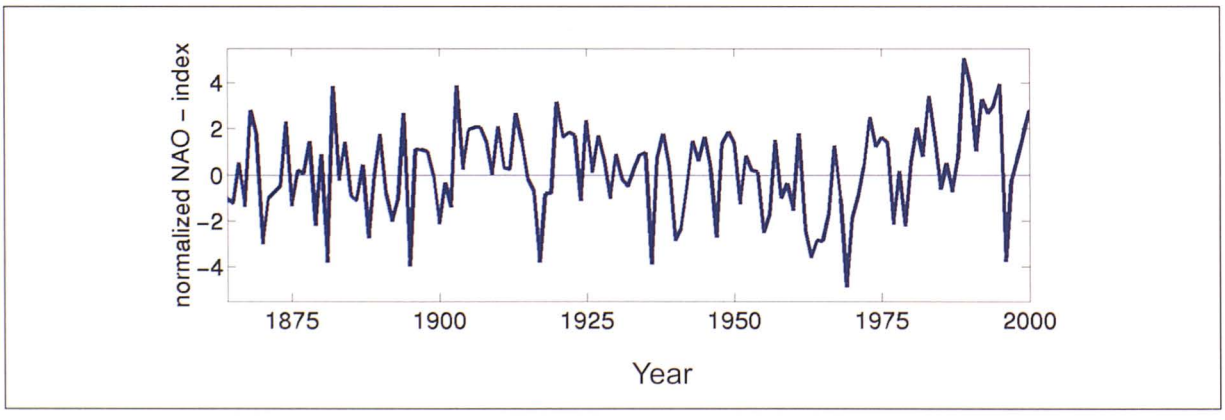

Figure 2.26 *Normalised time series of NAO index for winters (December-March) from 1864 to the present, based on data from Hurrell (http://www.met.rdg.ac.uk/cag/NAO/index.html)*

There have been many attempts to reconstruct the climate and the NAO of the past, employing historical weather records, tree ring data and ice core data [Appenzeller et al., 1998, and references therein]. Less work has been done with the AO, as it requires the pressure field of the whole hemisphere. There have been suggestions that the observed NAO/AO variation is a random or chaotic behaviour, which does not depend on external forcing [Christiansen, 2001; Stephenson et al., 2000]. This would mean that the observed NAO/AO long-term behaviour is natural variability. The other possibility implies an anthropogenic influence, i.e., that the currently observed NAO and AO change is a response to anthropogenic climate forcing [Hoerling et al., 2001; Paeth et al., 1999; Shindell et al., 1999].

2.7 CHANGES IN STRATOSPHERIC AEROSOLS SINCE THE 1970S.

The lower stratosphere, between the tropopause and about 30 km, contains a layer of aerosol particles, composed mainly of spherical droplets of sulphuric acid solution. Under background conditions (such as have pertained since 1996) the monomodal droplet size distribution peaks at radii of 50-80 nm and the aerosol layer often extends only to 25-27 km. Following a major volcanic eruption however, the total number of particles increases (up to a hundredfold), a population of larger particles (radii ~200-300 nm) is formed, and the layer extends above 30 km. Aerosol is important for a full understanding of the ozone layer for two reasons:

a) heterogeneous chemical reactions take place on aerosol surfaces – primarily conversion of N_2O_5 to HNO_3 but also, at temperatures <200 K, conversion of halogen reservoirs to free radicals.

b) aerosol affects radiative transfer in the stratosphere and thus impacts the dynamics (Section 2.5.1).

We present in this section the longest record of stratospheric aerosol measurements that exist in Europe – the lidar record at Garmisch-Partenkirchen (47.5°N, 11.1°E), which began in 1976 and which has been part of the NDSC since 1991. The lidar provides measurements of particle backscatter with high vertical resolution. A conversion model is used to calculate aerosol extinction, mass and surface from the backscatter data. This model is based on height and time-resolved aerosol size distributions derived from balloon-borne particle counter data from Laramie, Wyoming [Jäger and Hofmann, 1991; Jäger et al., 1995].

The lidar record of Figure 2.27 shows the integrated particle backscatter coefficient at 694.3 nm. Data are integrated from 1 km above the tropopause to the top of the aerosol layer at 30-35 km. The measurement density is several soundings per month. Volcanic eruptions of various magnitudes have been observed at this northern mid-latitude site: perturbations of global and long lasting significance (years) were caused by the equatorial eruptions of El Chichon (Mexico, 1982) and Pinatubo (Philippines, 1991), and hemispheric perturbations (of about 1 year) by the high latitude eruptions of St. Helens (USA, 1980) and Alaid (Kurile Islands, 1981). Other tropical eruptions causing diffuse backscatter increases were La Soufriere (Caribbean, 1979), Sierra Negra (Galapagos, 1979), Nyamuragira (Zaire, the "Mystery Cloud" of 1981), Nevado del Ruiz (Colombia, 1985) and Nyamuragira (Zaire, 1986), the latter two probably delaying the decay of the El Chichon perturbation. A further category is high latitude eruptions of only local significance which had no lasting effect on the lidar record but could be traced in individual backscatter profiles: Redoubt (Alaska, 1989), Kliuchevskoi (Kamchatka, 1994), and finally Shishaldin (Aleutian Islands, 1999).

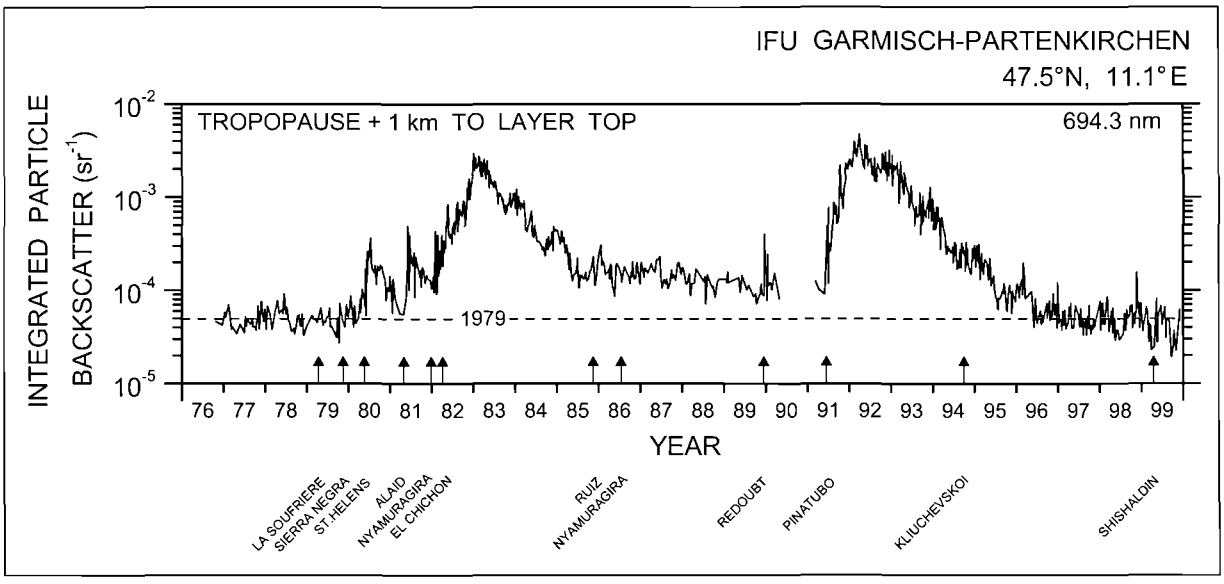

Figure 2.27 *Time variation of the integrated aerosol backscatter from lidar measurements of the stratospheric aerosol layer at northern hemisphere mid-latitudes. The dashed line indicates the 1979 mean. Volcanic eruptions are marked.*

This record of stratospheric particle load, which is typical for northern mid-latitudes, is characterised by two periods of increased volcanism and by three periods with little or no influence by volcanic eruptions, namely 1977 to 1979, 1989 to 1991, and 1997 up to the present time. The decay of the Pinatubo aerosol load terminated in 1996 when the 1979 background level was reached. In the background period prior to the Pinatubo eruption, however, a decay to values comparable with the late 1970s or 1990s could not be observed. Then Hofmann [1991] and Jäger [1994] discussed the possibility of anthropogenic influences contaminating the lower stratosphere. The return of the stratospheric aerosol load after the decay of the Pinatubo perturbation to values around the 1979 minimum indicates that any anthropogenic contribution to stratospheric aerosol must be far less than estimated in the previous EC assessment.